**Supporting information**

# Antiproliferative evaluation of mono- and disubstituted ferrocene derivatives with aldoxime ether- and ester-linked five-membered heterocycles

Martina Piškor Benković[1], Silvija Maračić[1], Mario Cetina[2], Dijana Jadreško[3], Sandra Kraljević Pavelić[4], Krešimir Pavelić[5] and Silvana Raić-Malić[1*]

[1] Department of Organic Chemistry, University of Zagreb Faculty of Chemical Engineering and Technology, Marulićev trg 20, 10000 Zagreb, Croatia

[2] Department of Applied Chemistry, University of Zagreb Faculty of Textile Technology, Prilaz Baruna Filipovića 28a, 10000 Zagreb, Croatia

[3] Division for Marine and Environmental Research, Ruđer Bošković Institute, Zagreb 10000, Croatia

[4] University of Rijeka Faculty of Health Studies, Viktora Cara Emina 5, 51000 Rijeka, Croatia

[5] Juraj Dobrila University of Pula Faculty of Medicine, 52100 Pula, Croatia

## Content

**1. NMR spectra of novel compounds** ..... 2

1.1. NMR spectra of novel alkynyl derivatives **2a–c**, **3b**, **3c**, **3e** and **3f** ..... 2

1.2. NMR spectra of novel monosubstituted ferrocene-heterocycle hybrids **5a–c**, **6a–f** ..... 9

1.3. NMR spectra of novel disubstituted ferrocene-heterocycle hybrids **8a–c**, **9a–f** ..... 18

**2. HRMS spectra of novel compounds 5a–c, 6a–f, 8a–c, 9a–f** ..... 27

**3. X-ray crystal structure studies** ..... 36

3.1 Experimental ..... 36

3.2. Results and discussion ..... 38

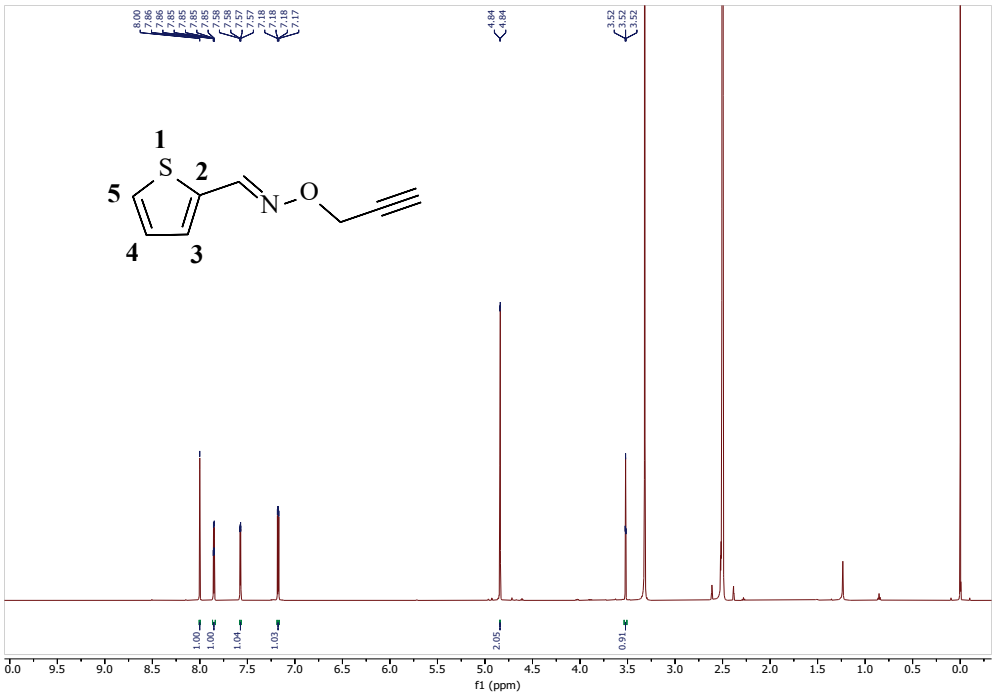
**4. References** ..... 44

## 1. NMR spectra of novel compounds

1.1. NMR spectra of novel alkynyl derivatives **2a–c**, **3b**, **3c**, **3e** and **3f**

**Figure S1.** a) $^{1}$H NMR and b) $^{13}$C (APT) NMR spectra of compd. **2a**

a)




b)

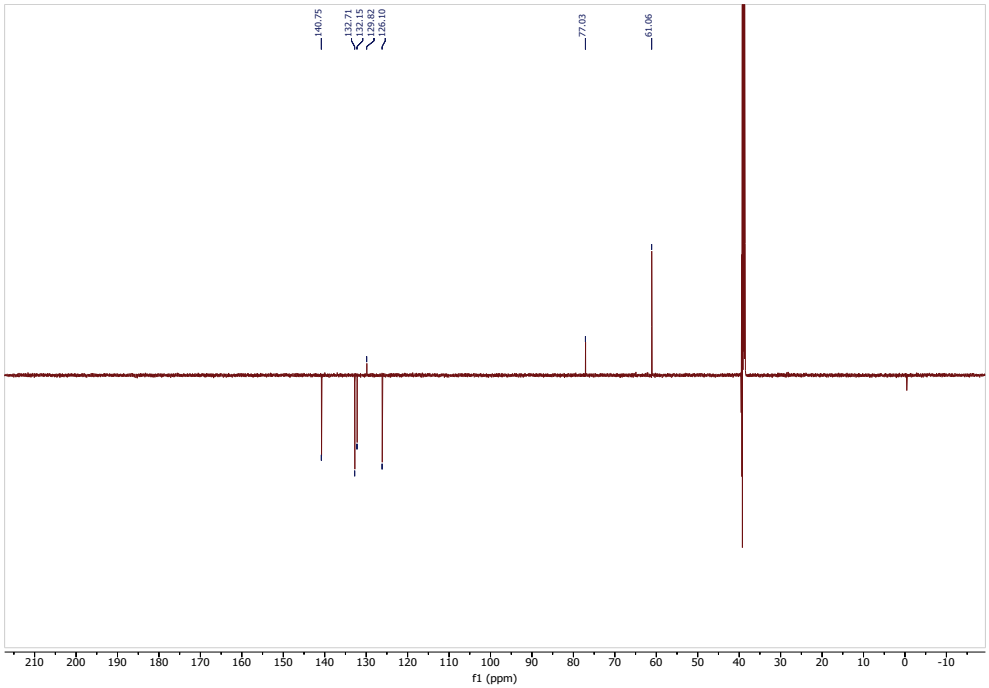
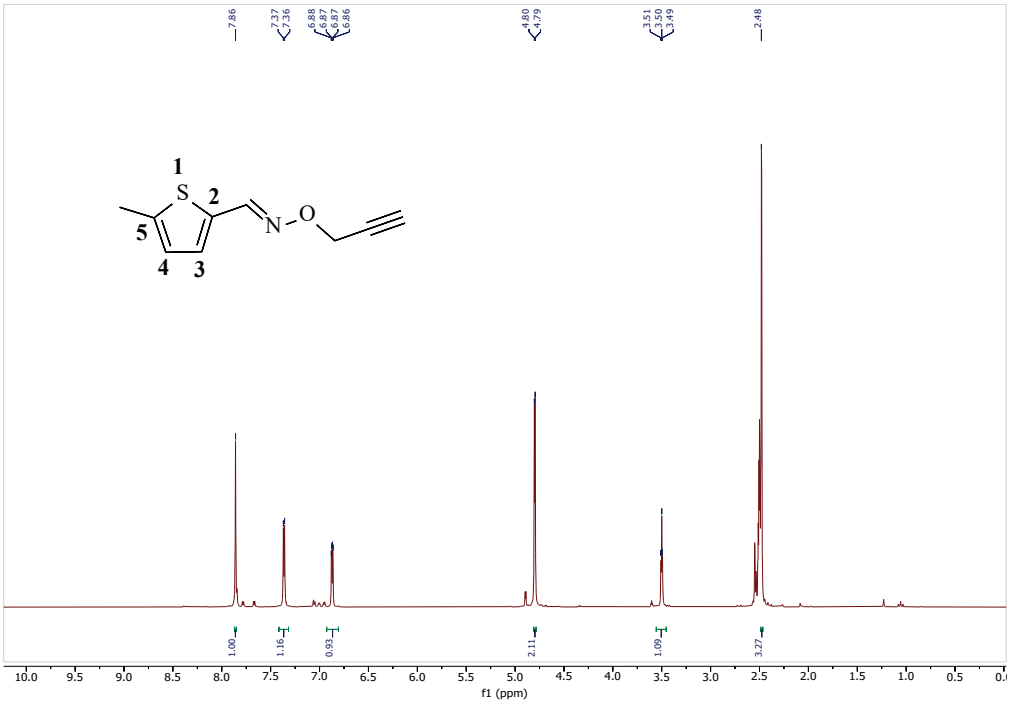


**Figure S2.** a) $^{1}$H NMR and b) $^{13}$C NMR spectra of compd. **2b**

a)




b)

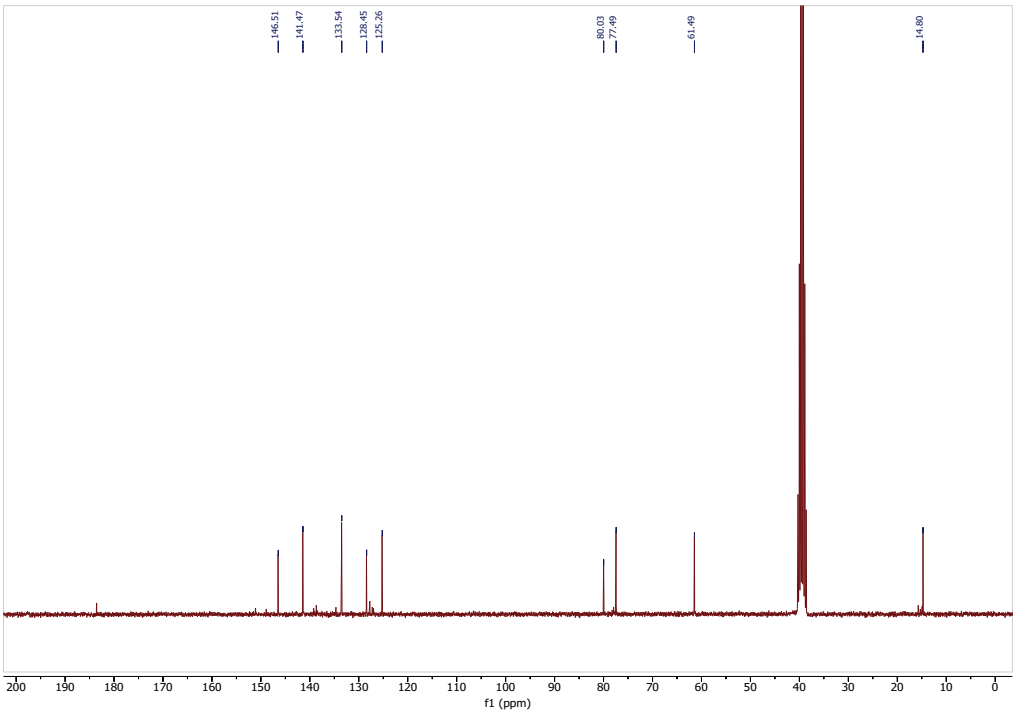
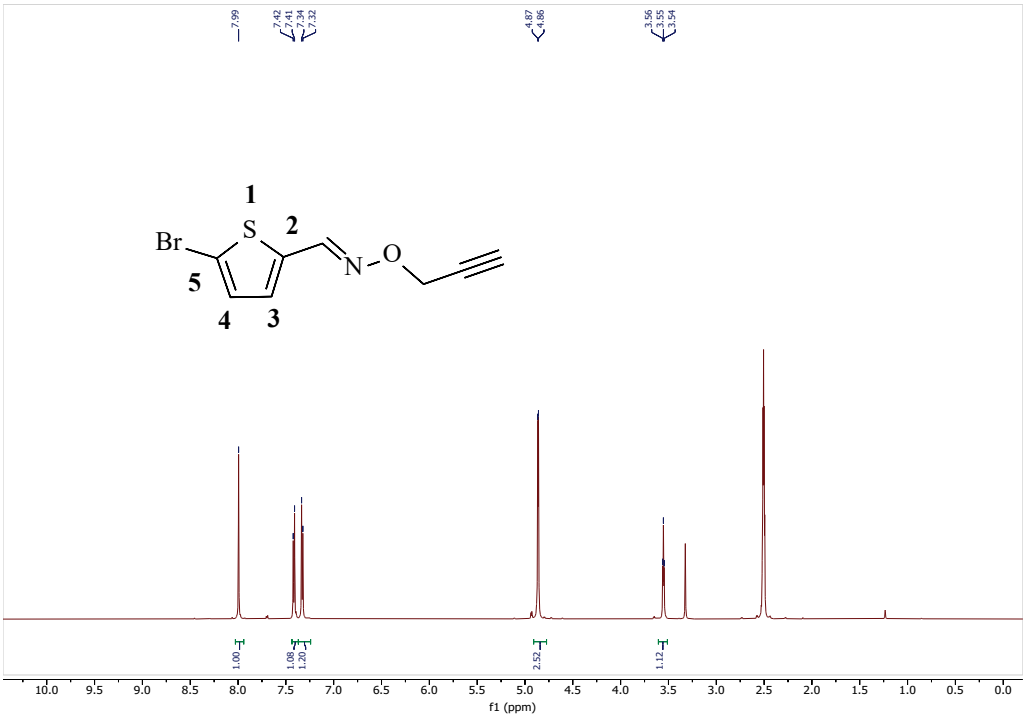


**Figure S3.** a) $^{1}H$ NMR and b) $^{13}C$ NMR spectra of compd. **2c**

**a)**




**b)**

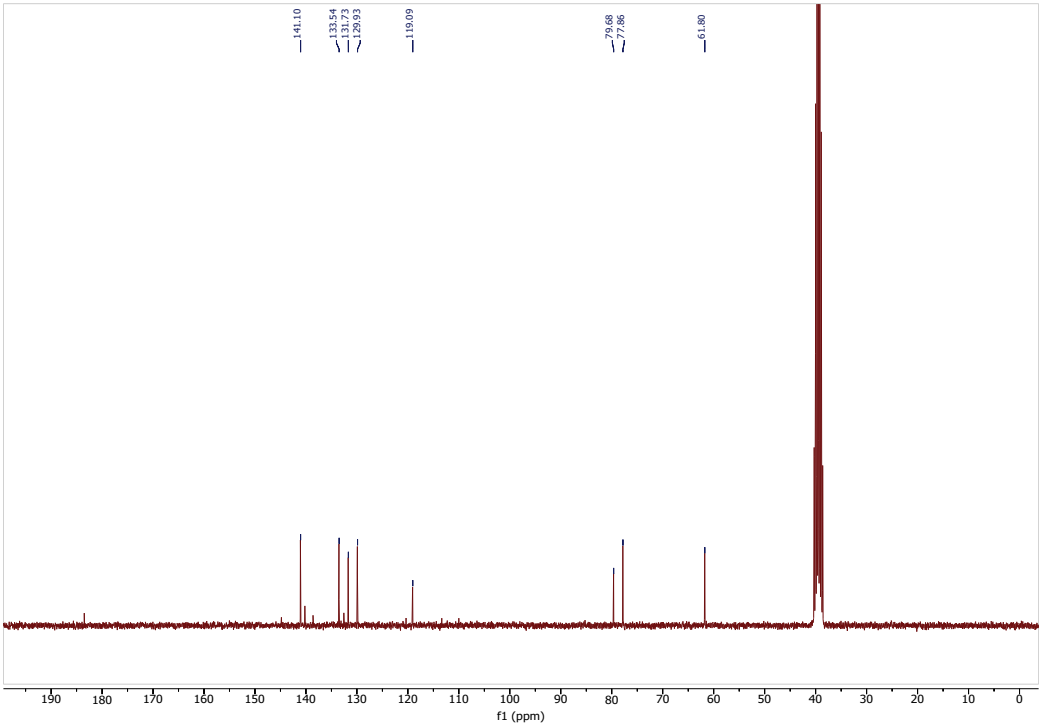
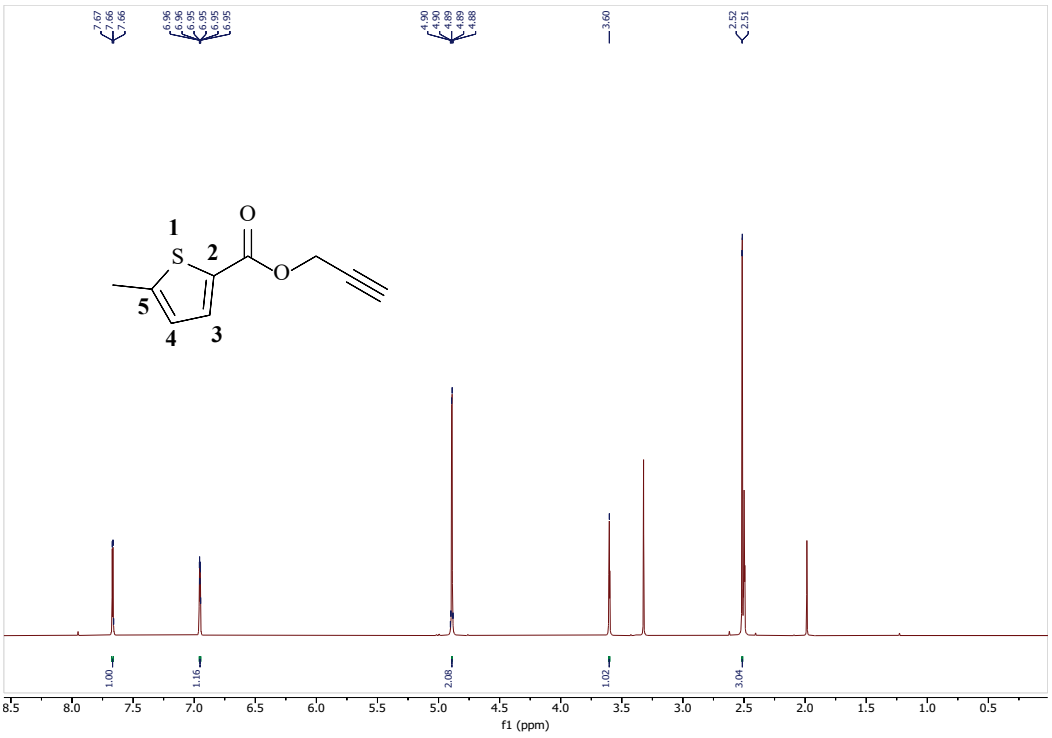


**Figure S4.** a) $^{1}H$ NMR and b) $^{13}C$ (APT) NMR spectra of compd. **3b**

**a)**




**b)**

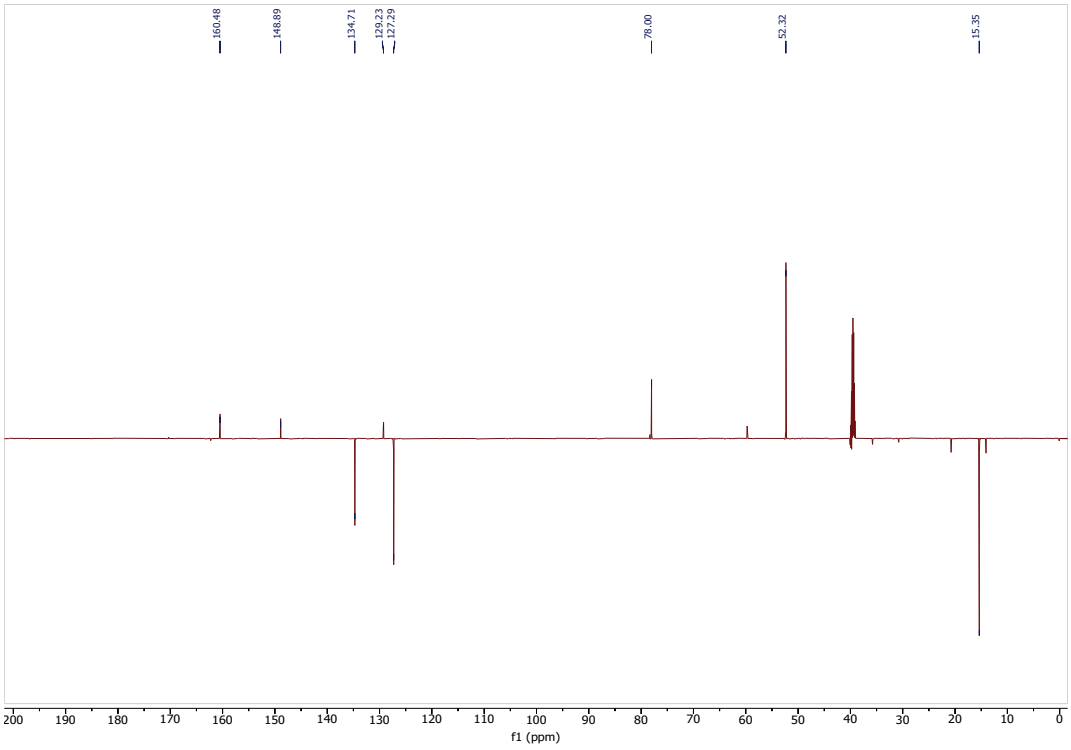
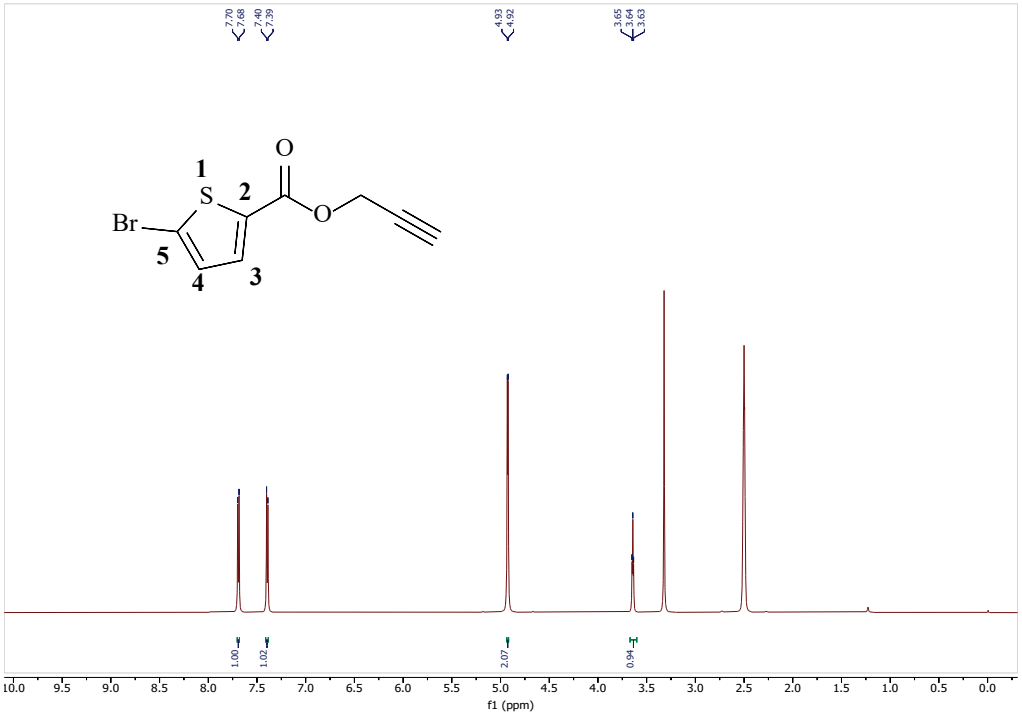


**Figure S5.** a) $^{1}$H NMR and b) $^{13}$C (APT) NMR spectra of compd. **3c**

**a)**




**b)**

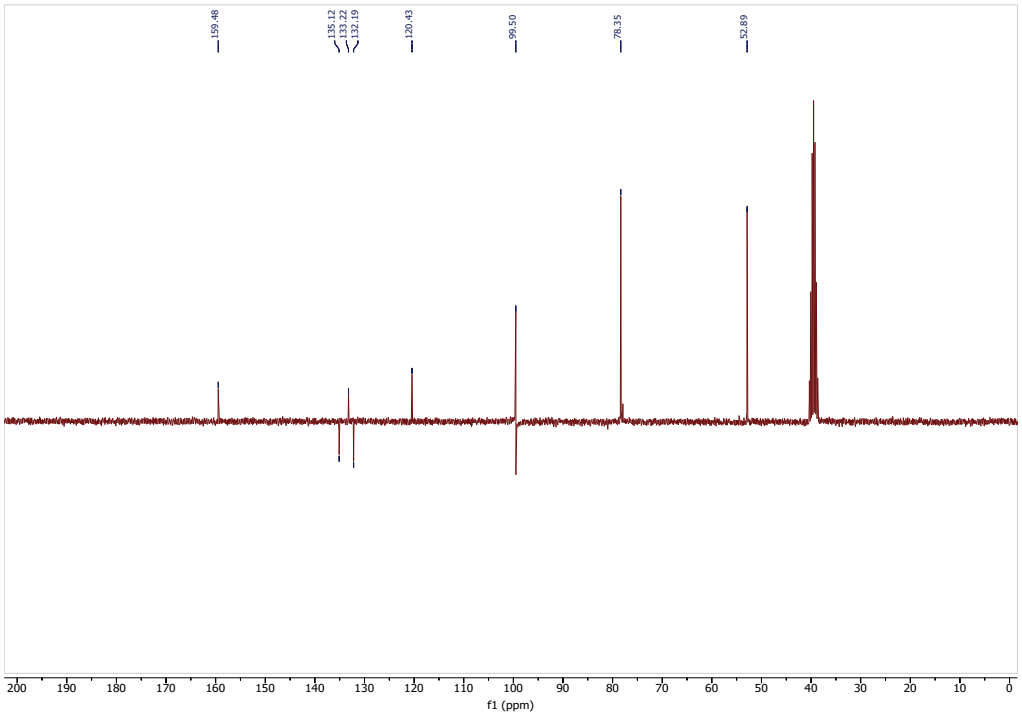
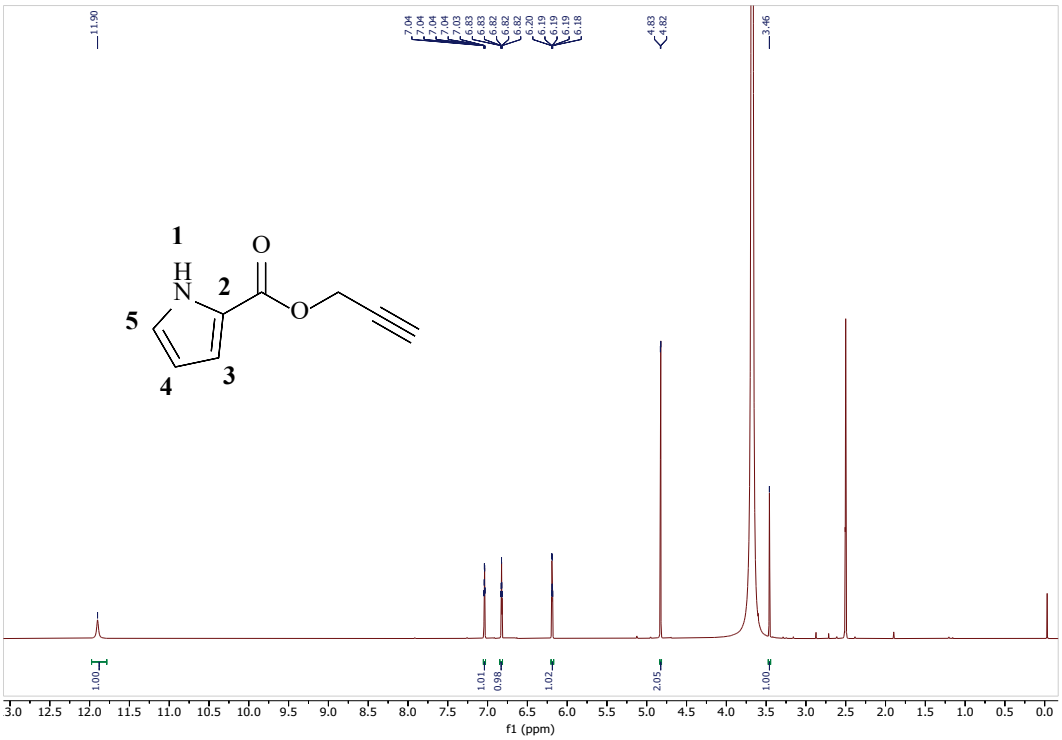


**Figure S6.** a) $^{1}$H NMR and b) $^{13}$C (APT) NMR spectra of compd. **3e**

a)




b)

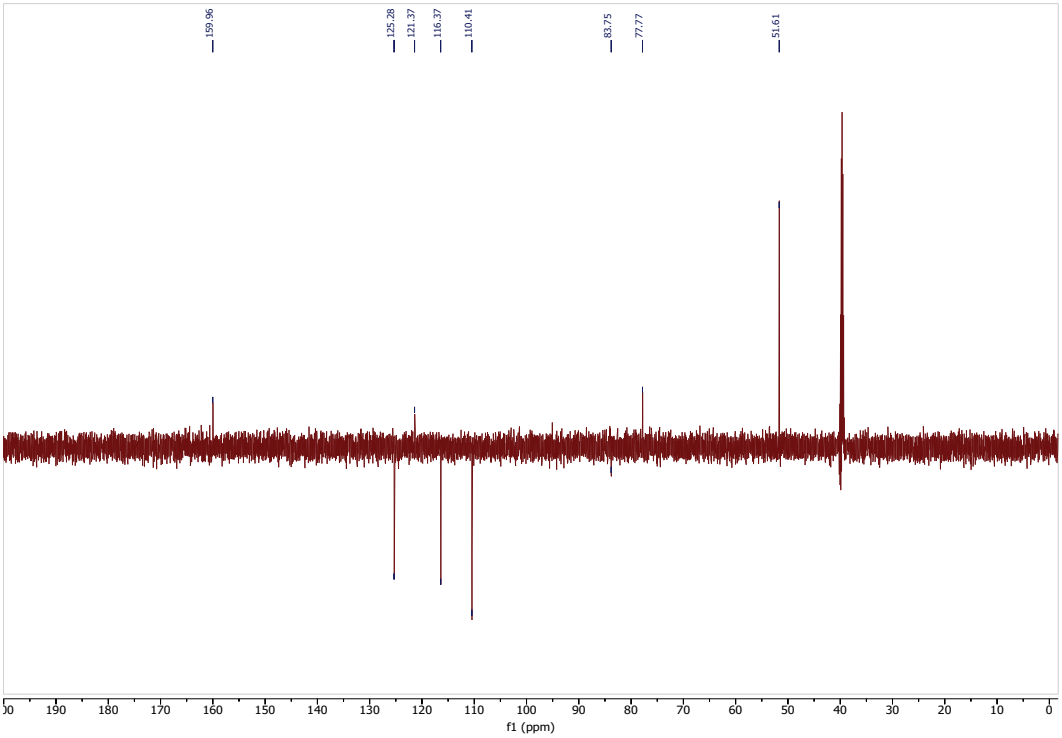
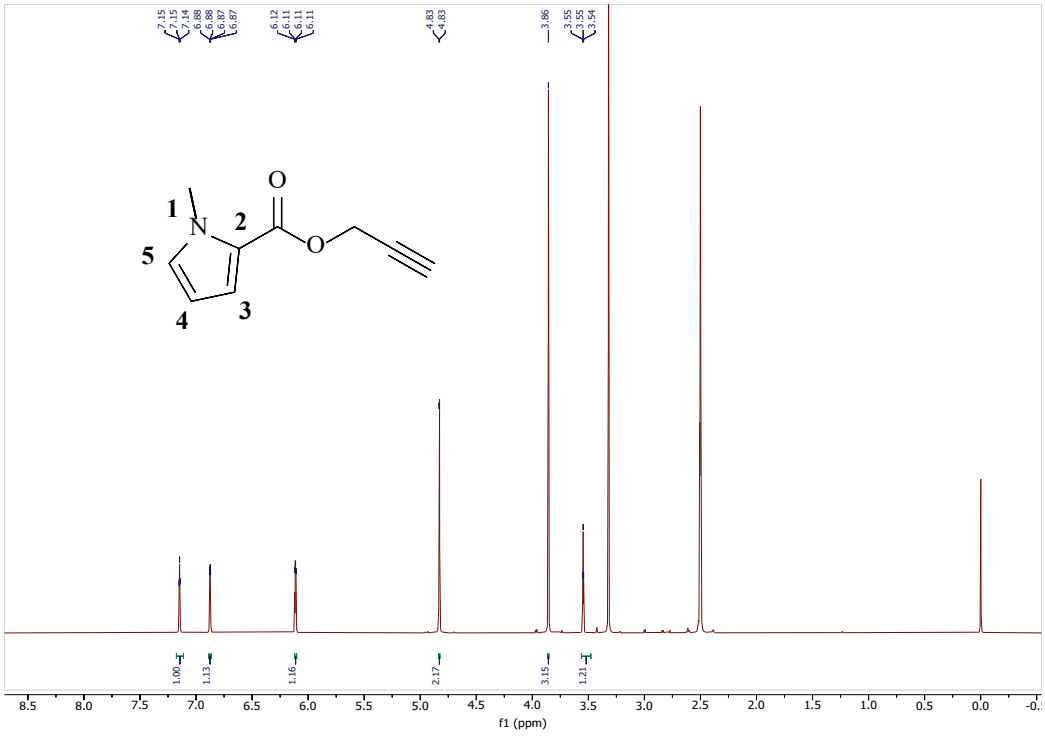
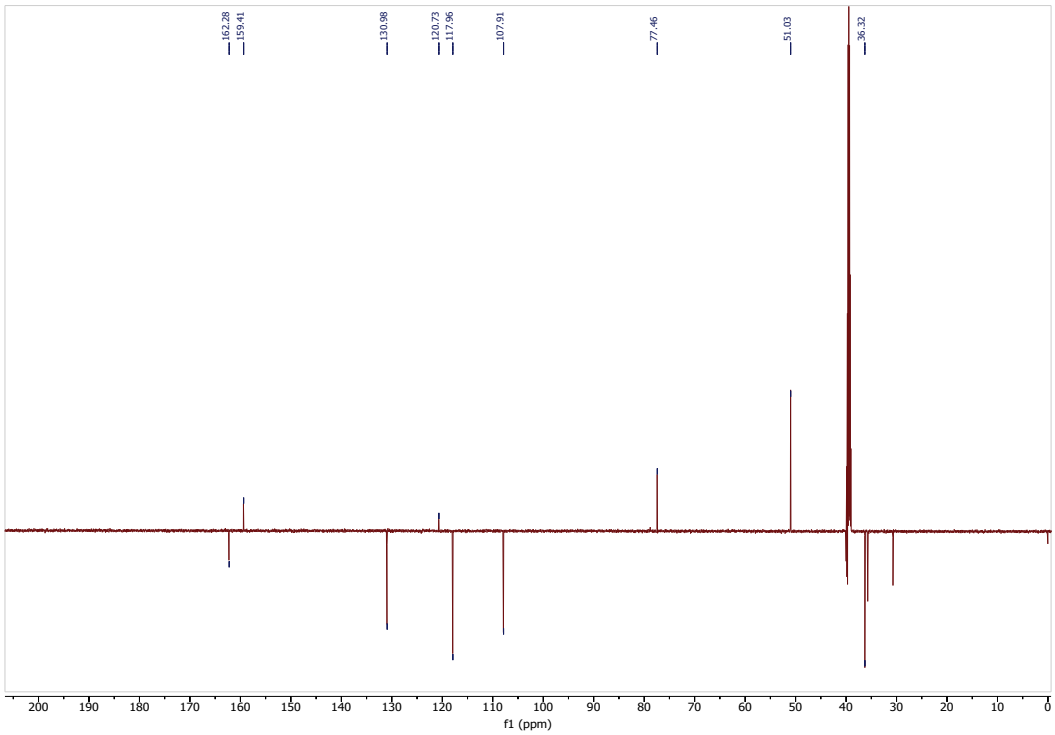


**Figure S7.** a) $^{1}H$ NMR and b) $^{13}C$ (APT) NMR spectra of compd. **3f**

a)



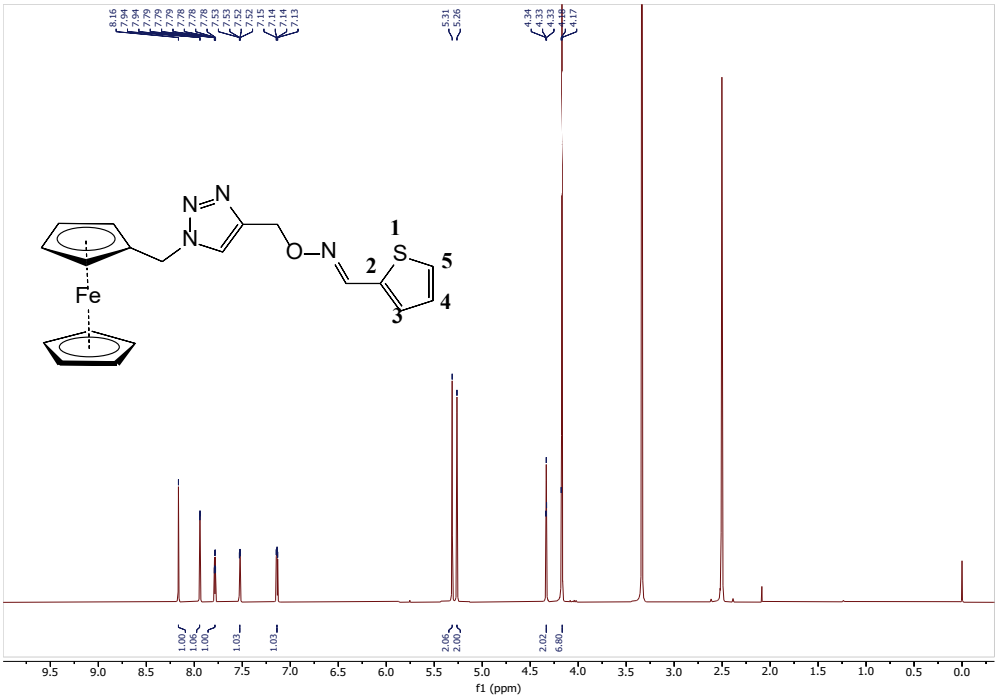

b)



1.2. NMR spectra of novel monosubstituted ferrocene-heterocycle hybrids **5a–c**, **6a–f**

**Figure S8.** a) $^{1}$H NMR and b) $^{13}$C (APT) NMR spectra of compd. **5a**

a)




b)

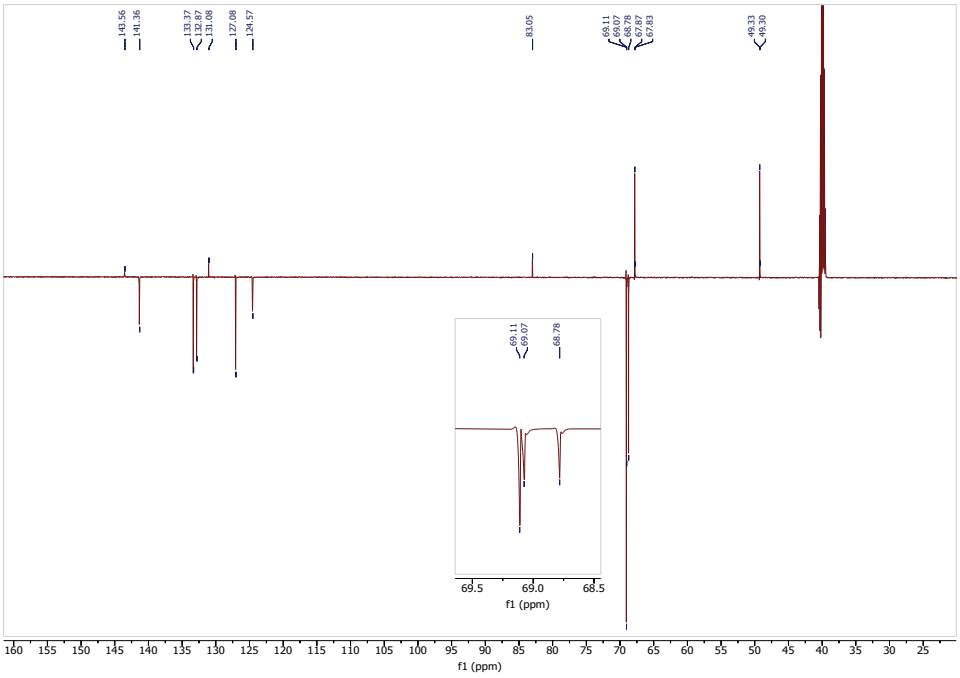
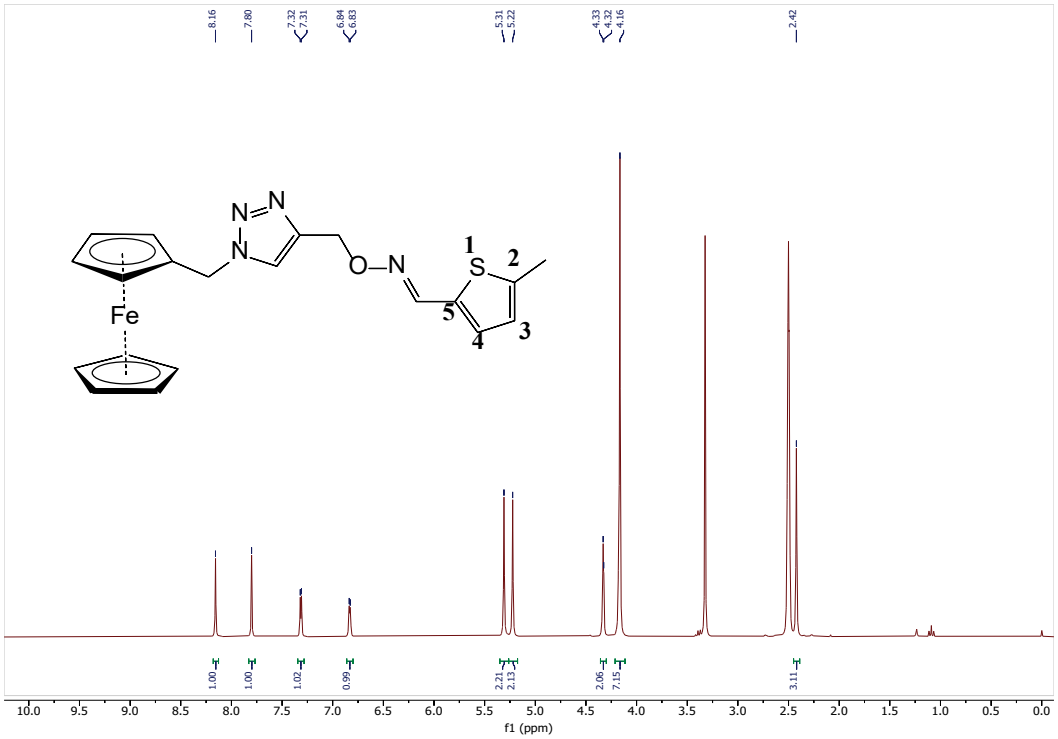


**Figure S9.** a) $^{1}$H NMR and b) $^{13}$C (APT) NMR spectra of compd. **5b**

a)




b)

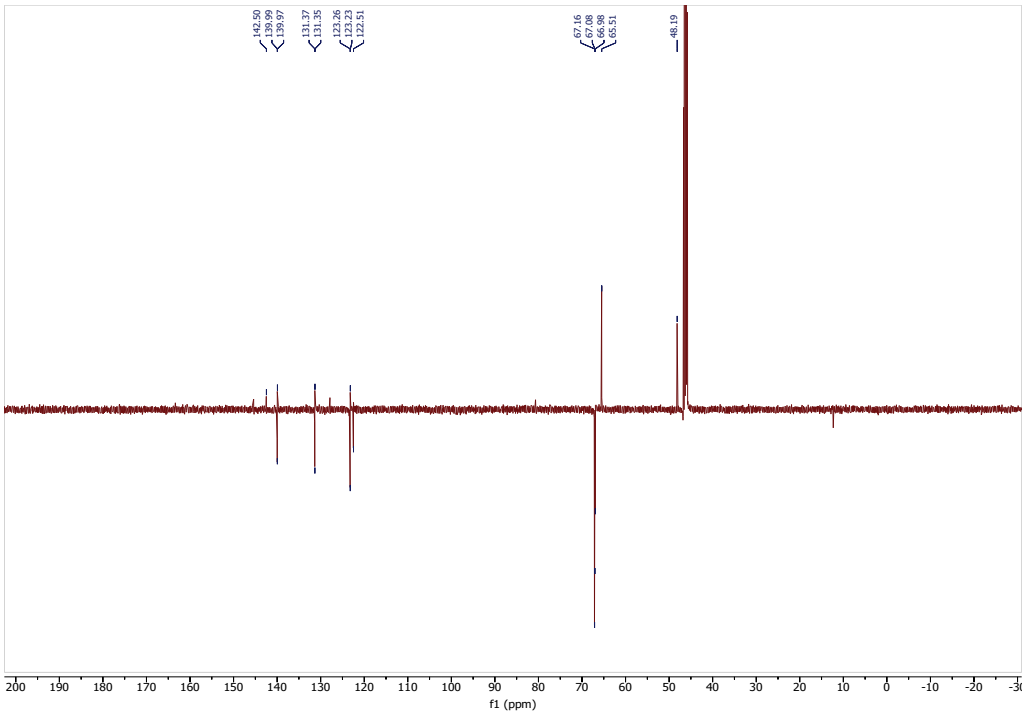
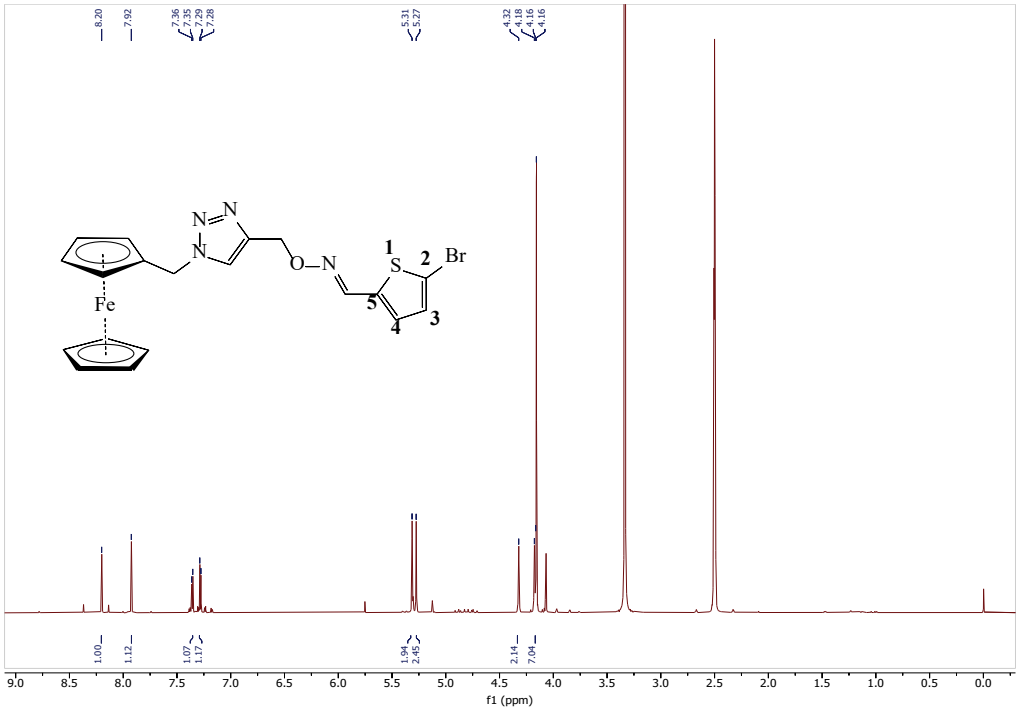


**Figure S10.** a) $^{1}$H NMR and b) $^{13}$C (APT) NMR spectra of compd. **5c**

**a)**




**b)**

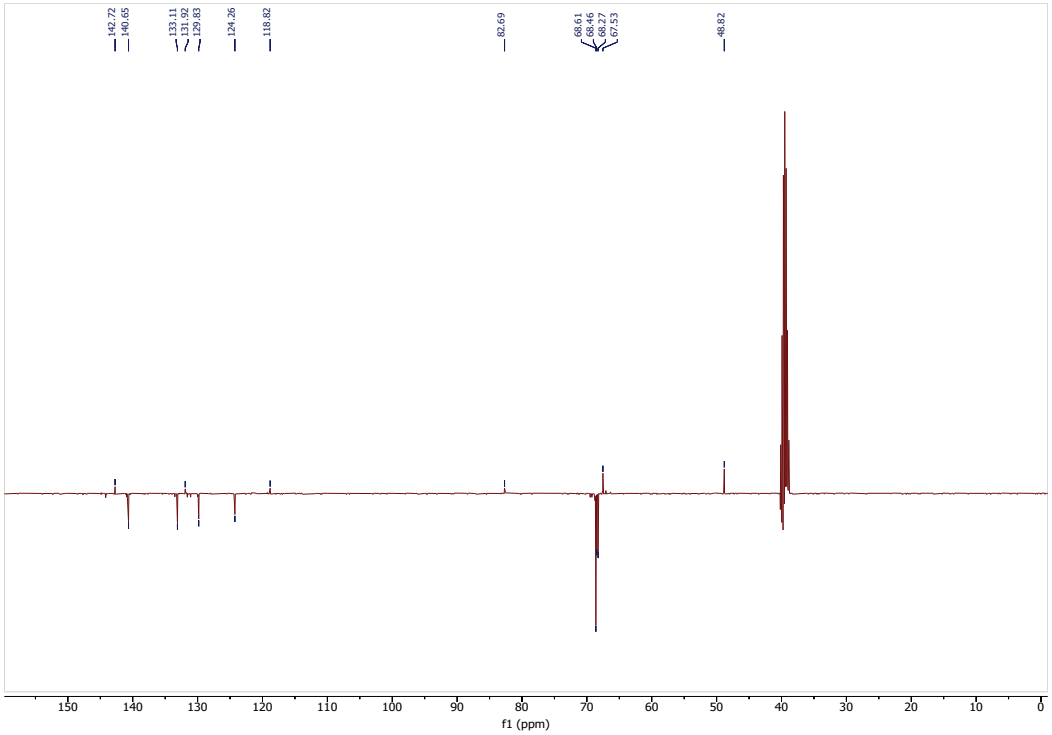
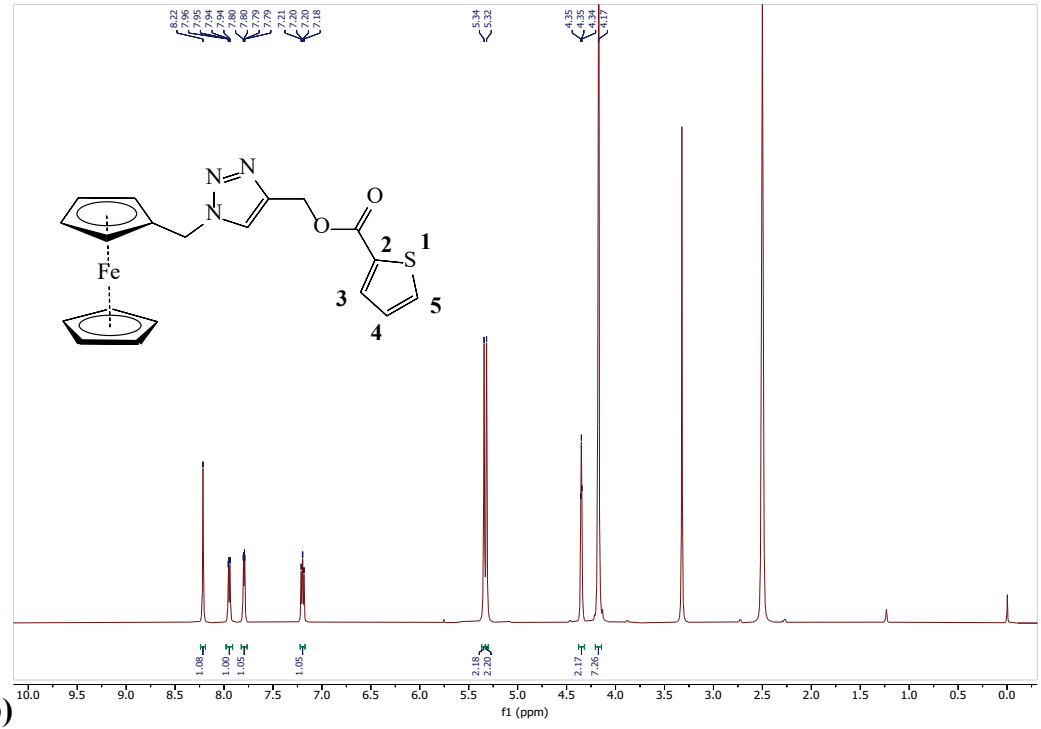


**Figure S11.** a) $^{1}$H NMR and b) $^{13}$C (APT) NMR spectra of compd. **6a**

**a)**




**b)**

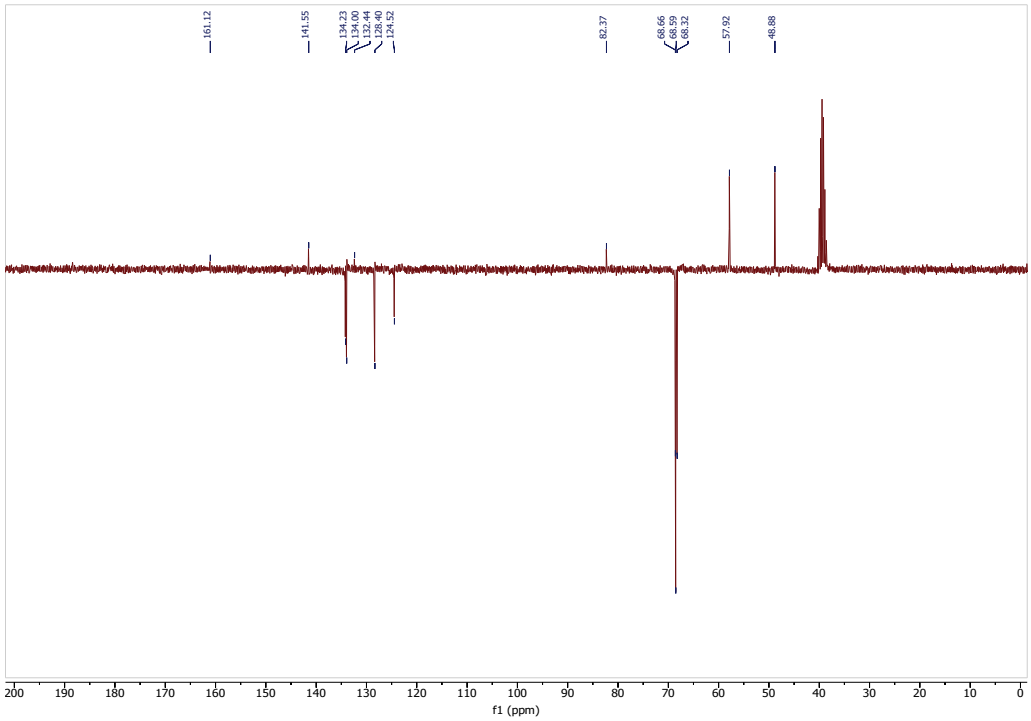
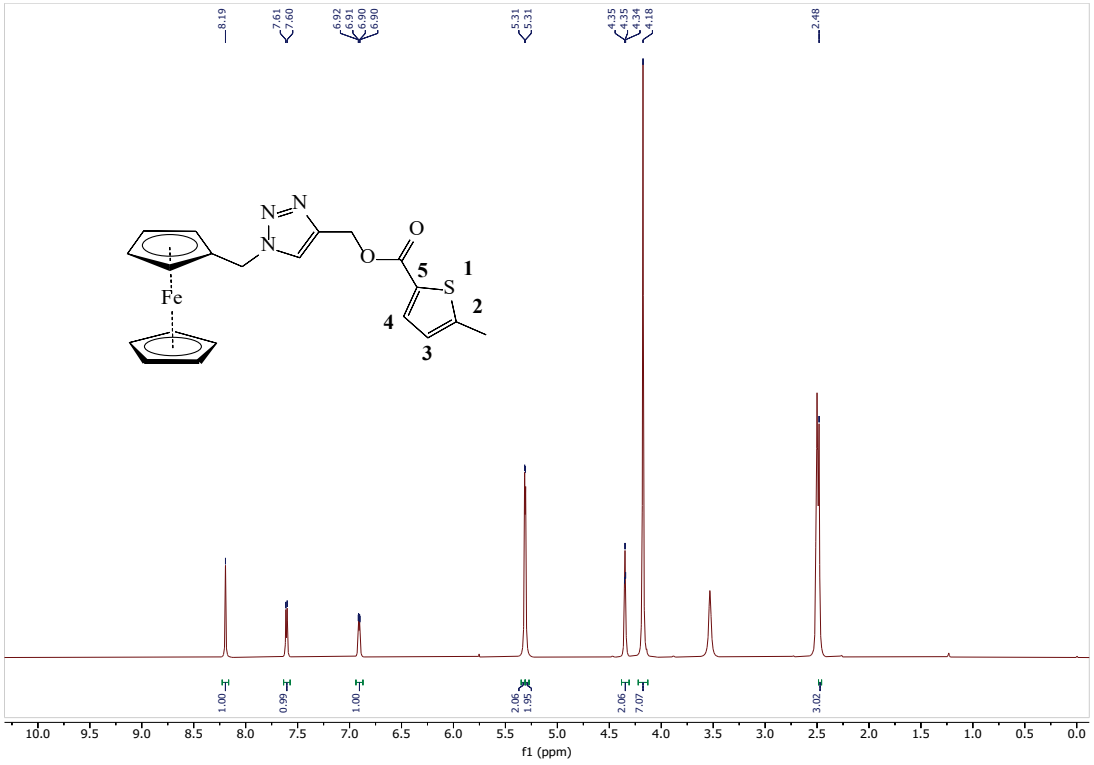


**Figure S12.** a) $^{1}$H NMR and b) $^{13}$C NMR spectra of compd. **6b**

**a)**




**b)**

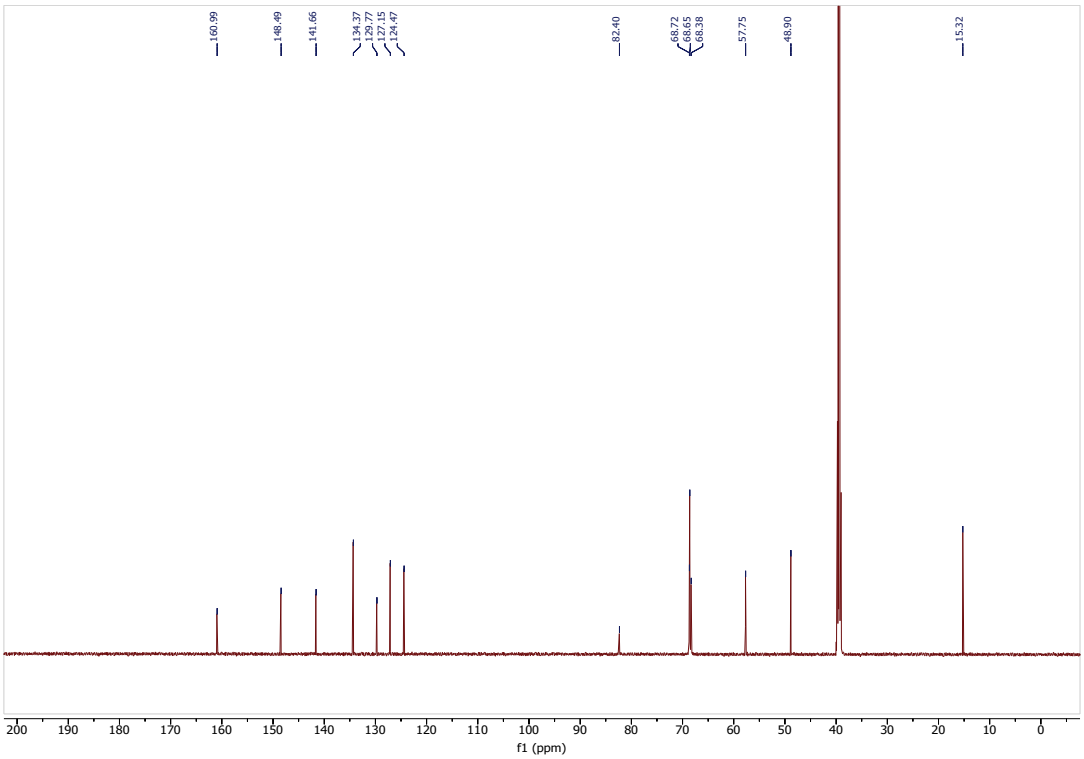
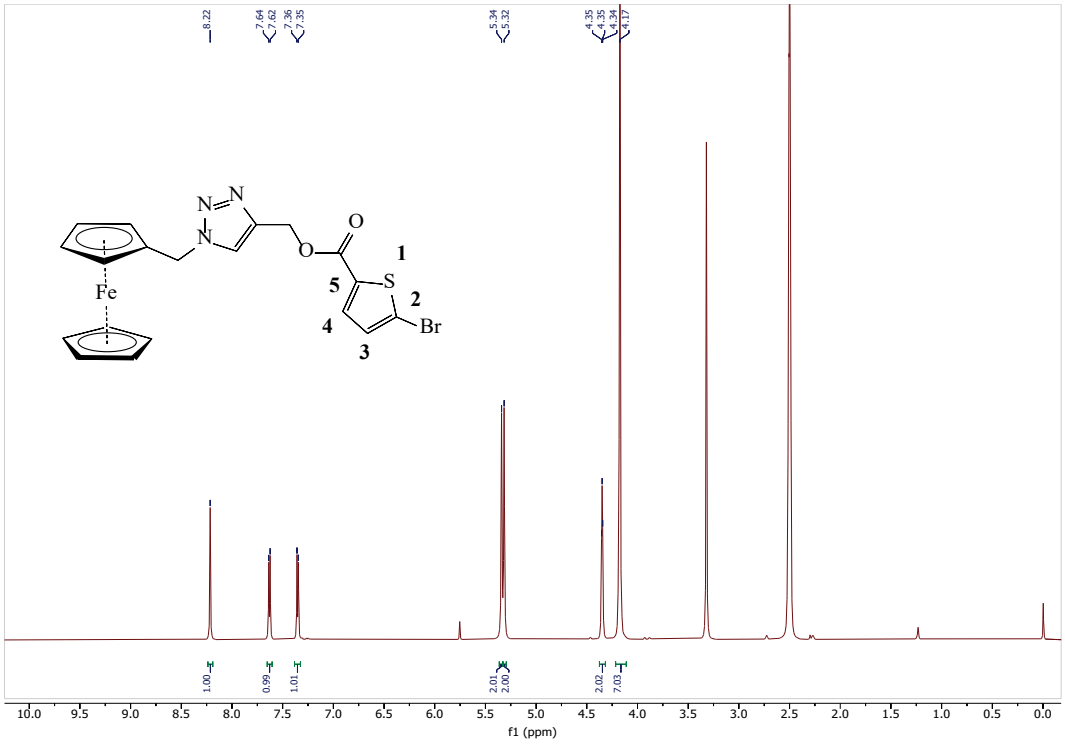


**Figure S13.** a) a) $^{1}$H NMR and b) $^{13}$C (APT) NMR spectra of compd. **6c**

**a)**




**b)**

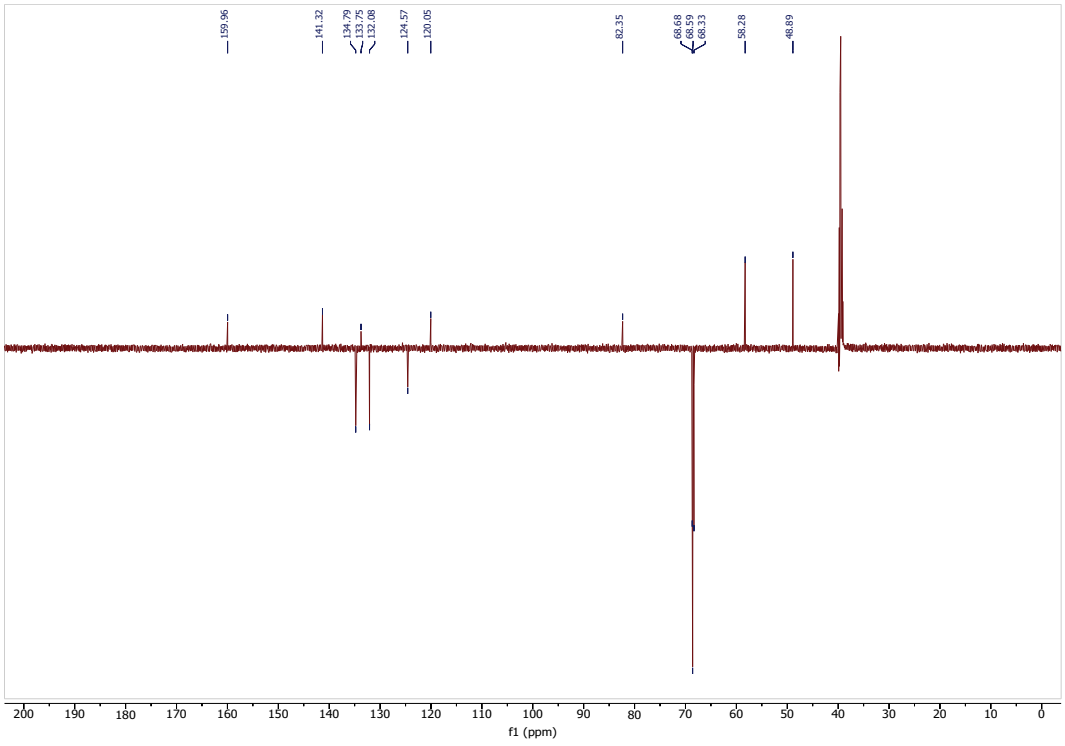
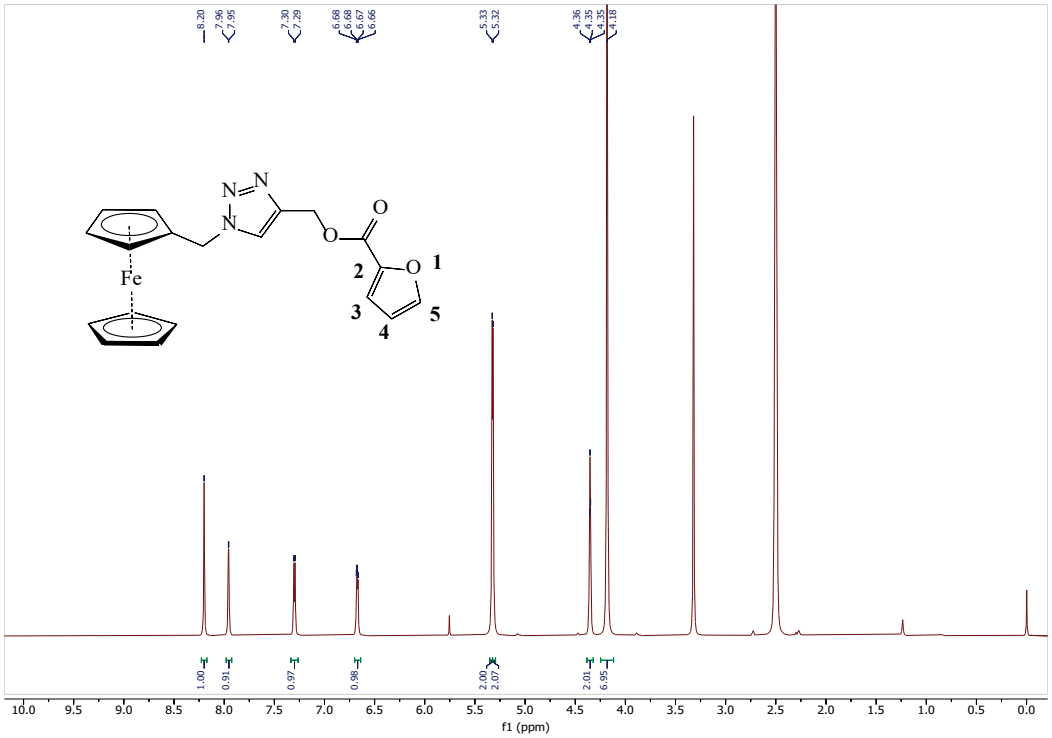


**Figure S14.** a) $^{1}$H NMR and b) $^{13}$C (APT) NMR spectra of compd. **6d**

**a)**




b)

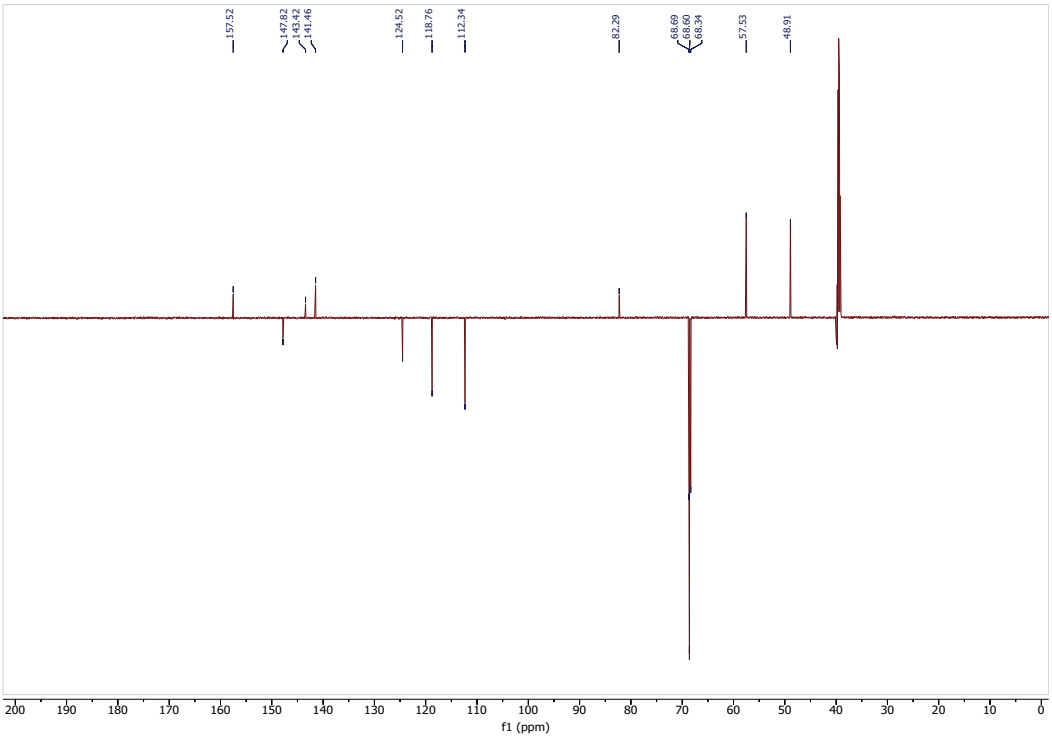
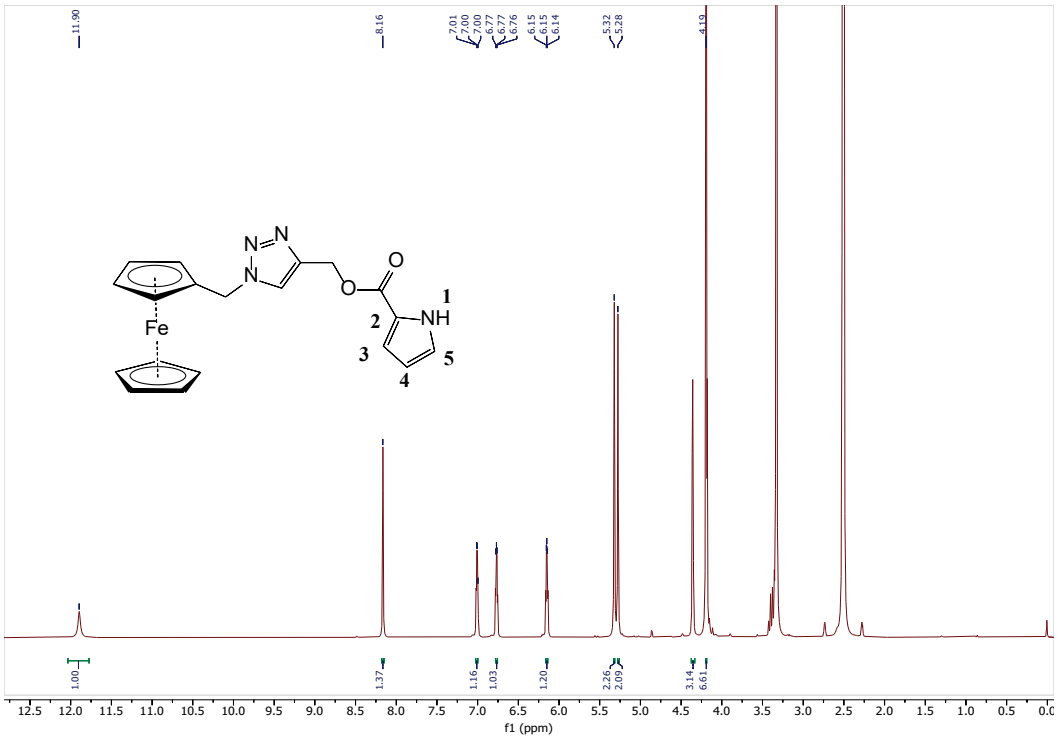


**Figure S15.** a) $^{1}$H NMR and b) $^{13}$C (APT) NMR spectra of compd. **6e**

**a)**




**b)**

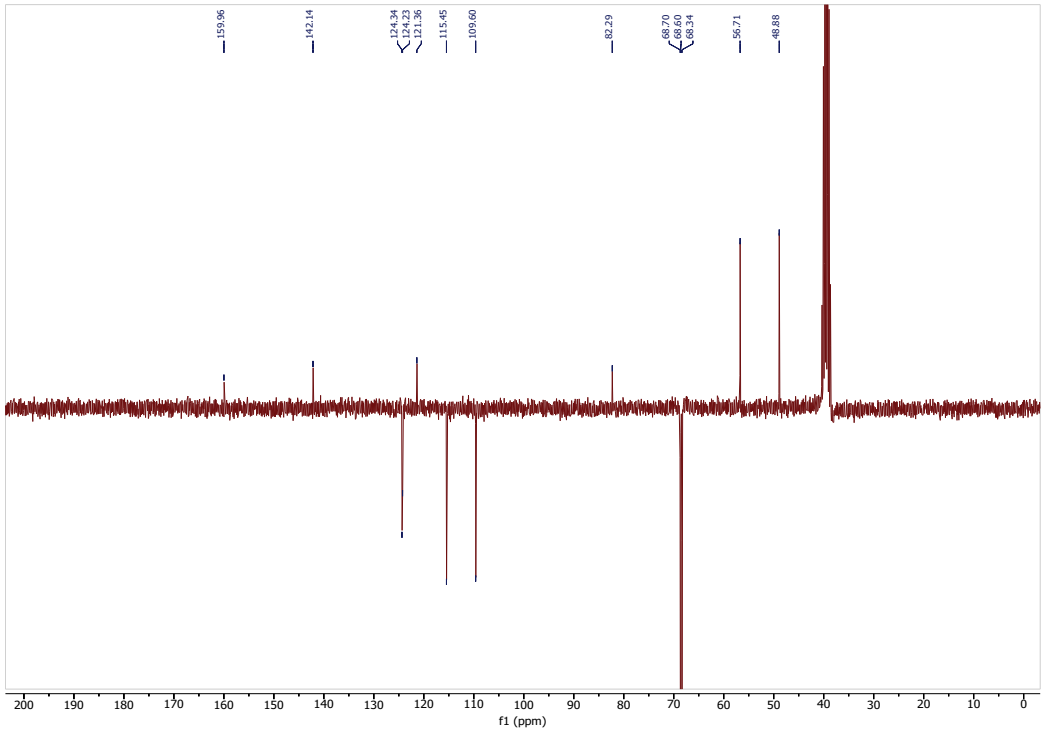
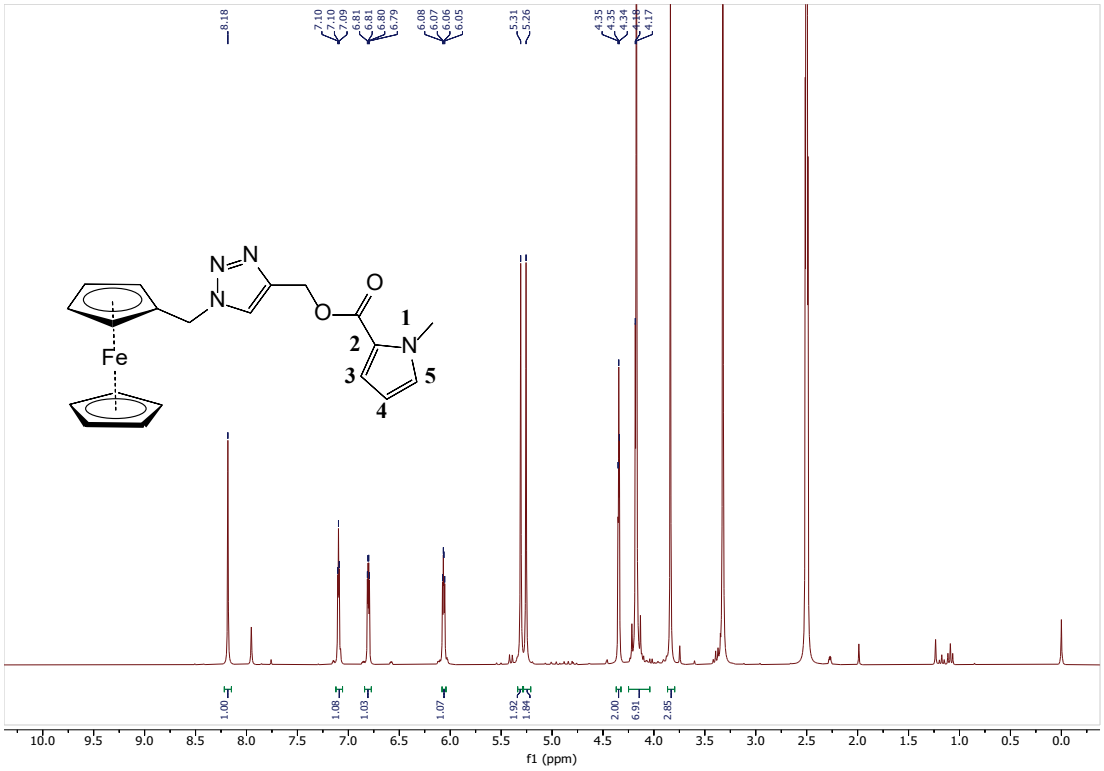
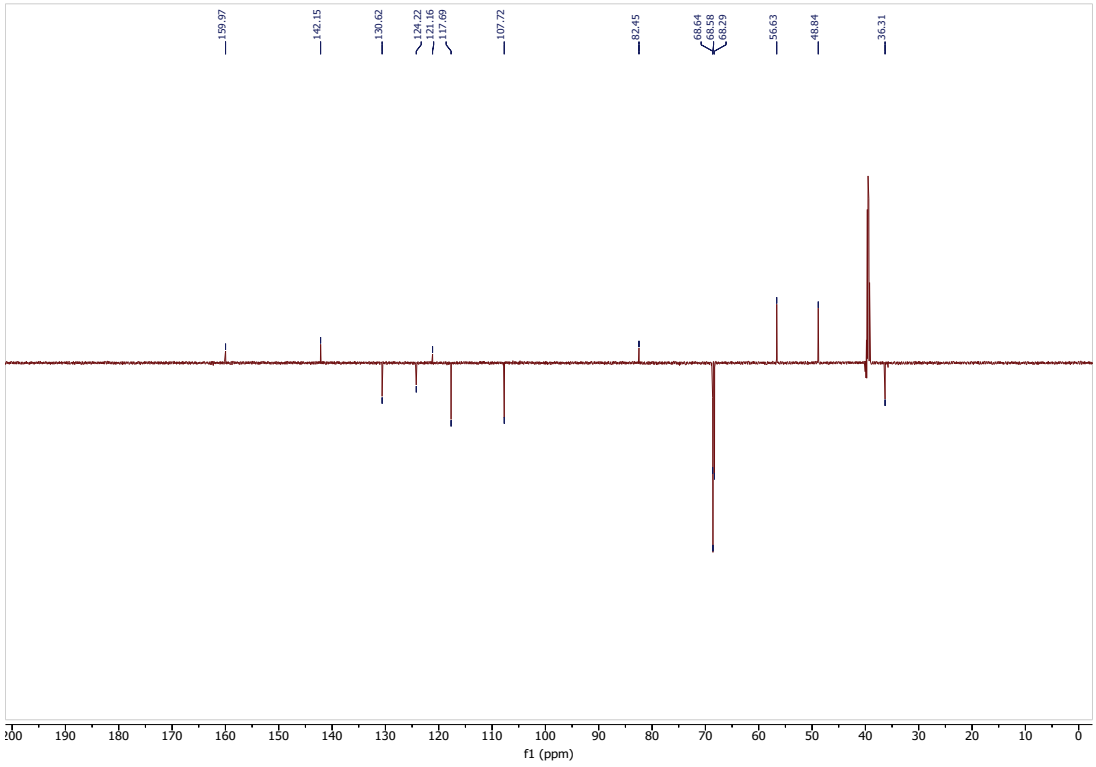


**Figure S16.** a) $^{1}$H NMR and b) $^{13}$C (APT) NMR spectra of compd. **6f**

**a)**



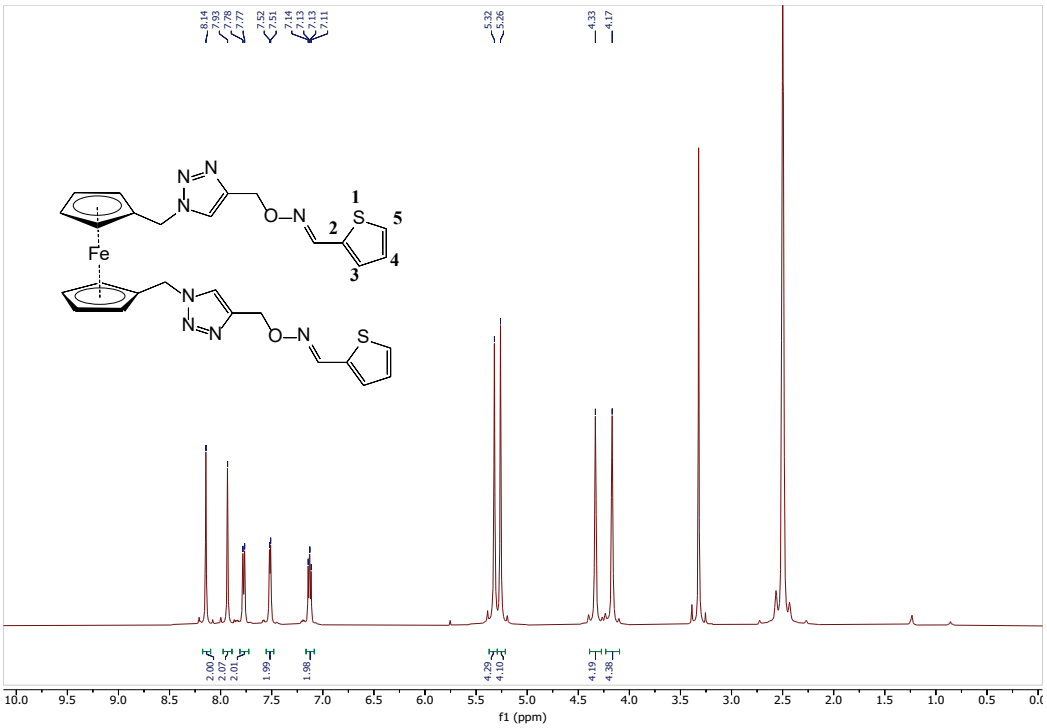

**b)**



1.3. NMR spectra of novel disubstituted ferrocene-heterocycle hybrids **8a–c**, **9a–f**

**Figure S17.** a) $^{1}$H NMR and b) $^{13}$C (APT) NMR spectra of compd. **8a**

a)




b)

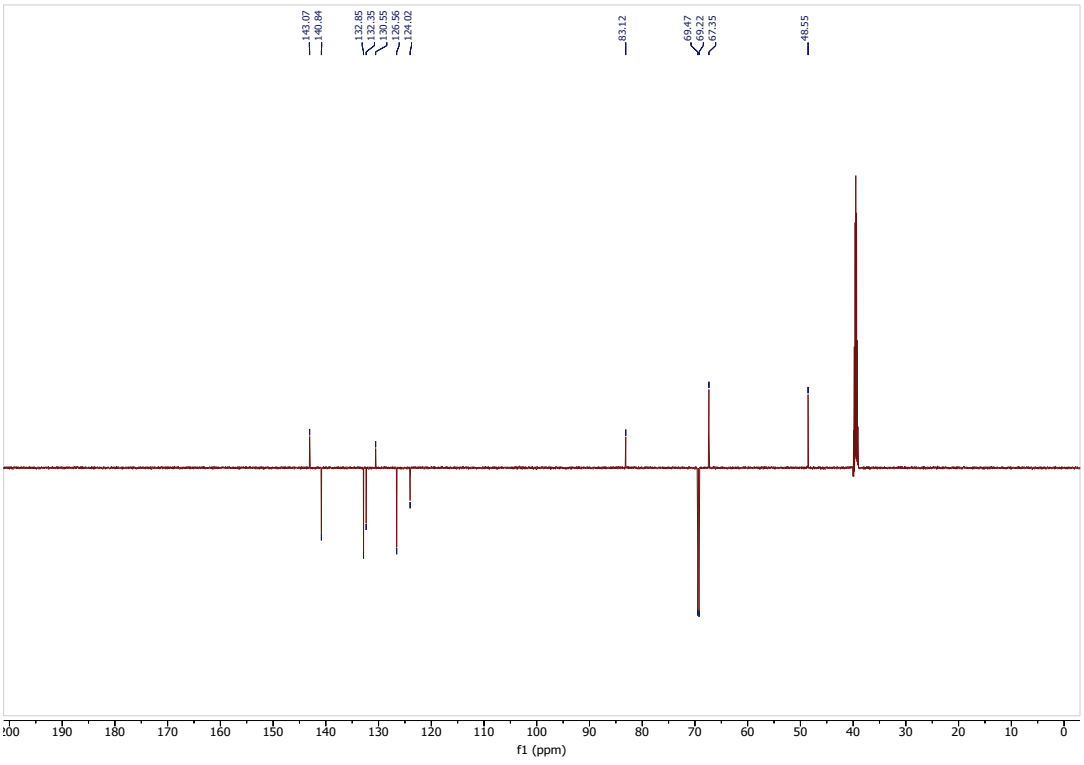
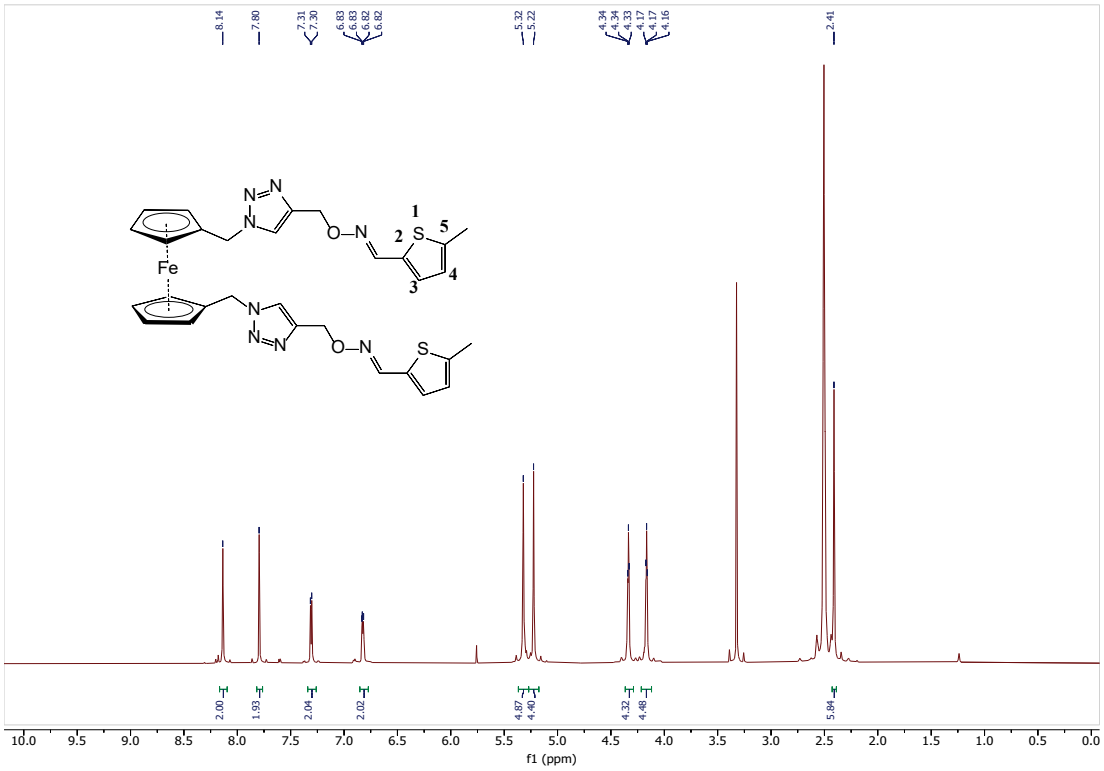


**Figure S18.** a) $^{1}$H NMR and b) $^{13}$C (APT) NMR spectra of compd. **8b**

**a)**




**b)**

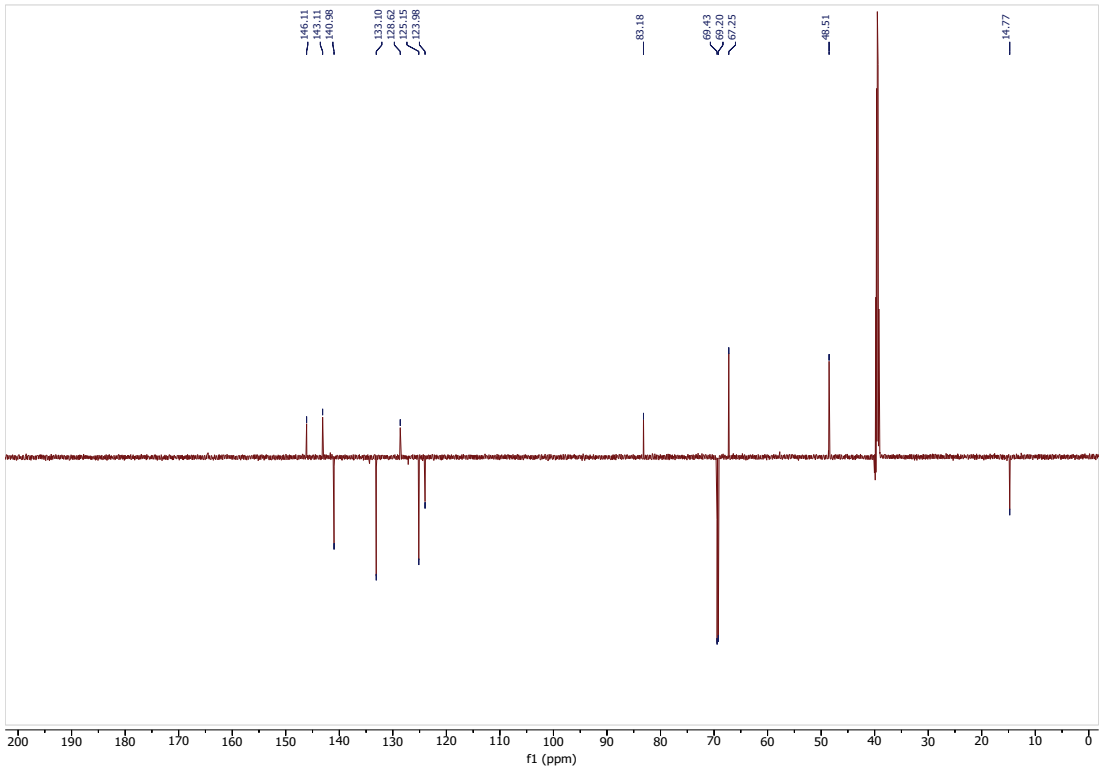
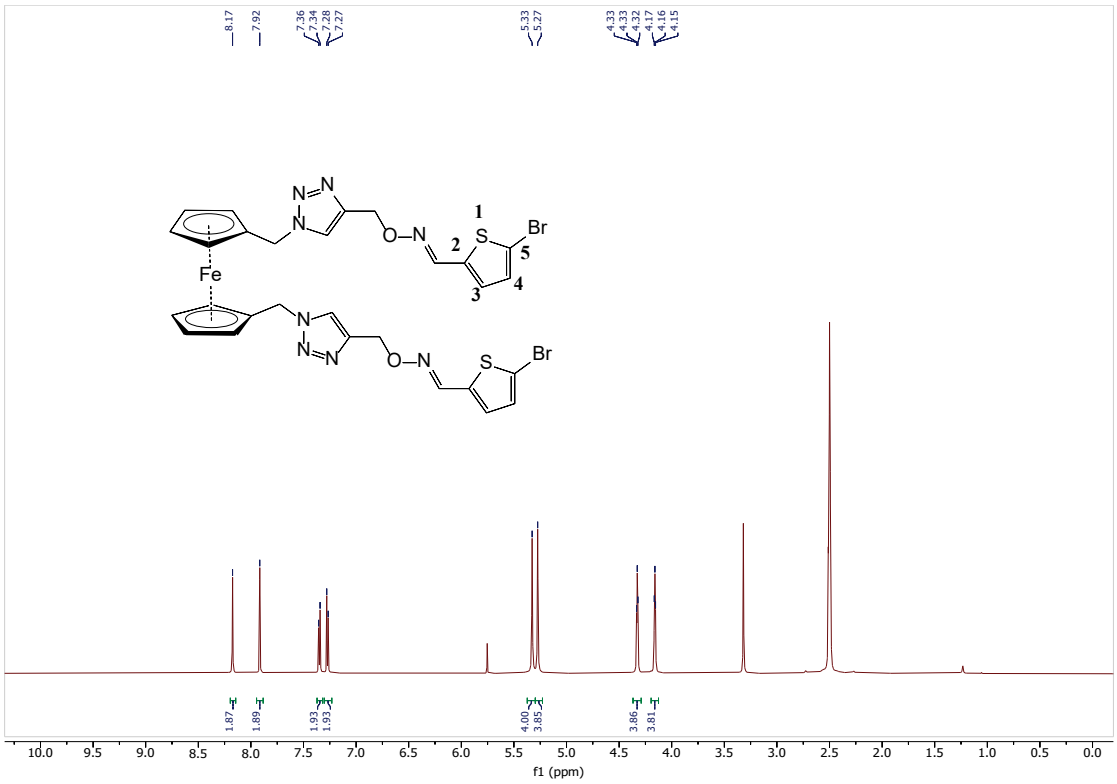


**Figure S19.** a) $^{1}$H NMR and b) $^{13}$C NMR spectra of compd. **8c**

**a)**




**b)**

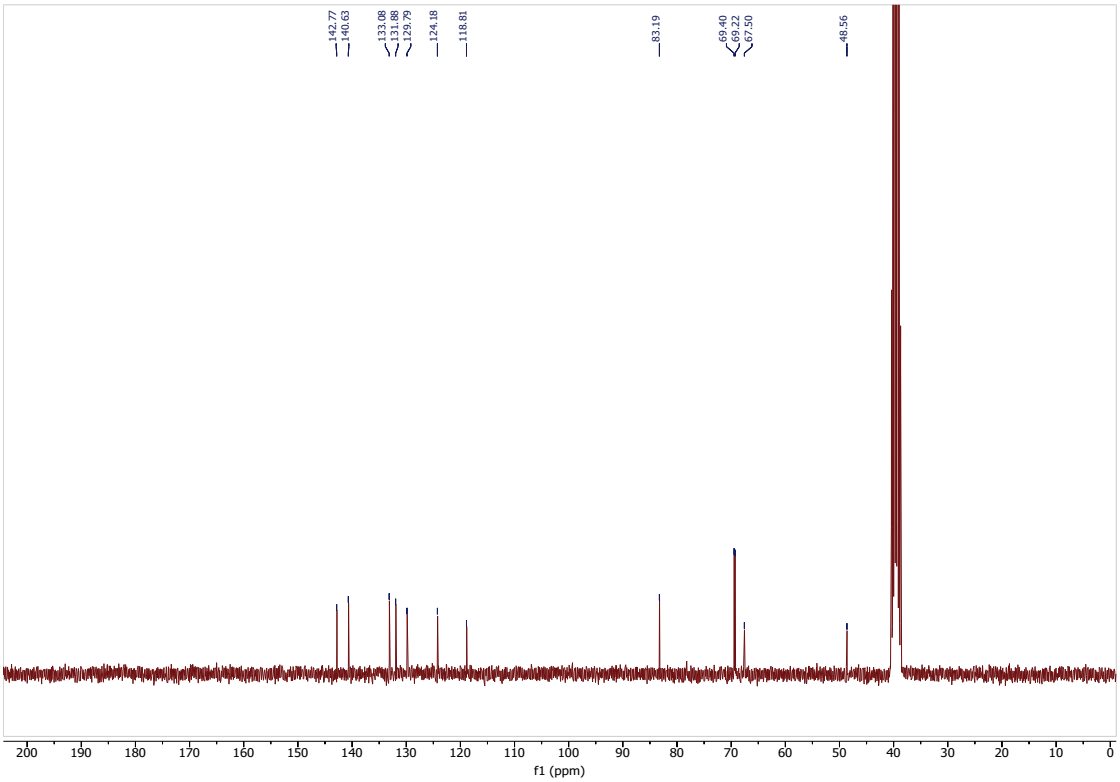
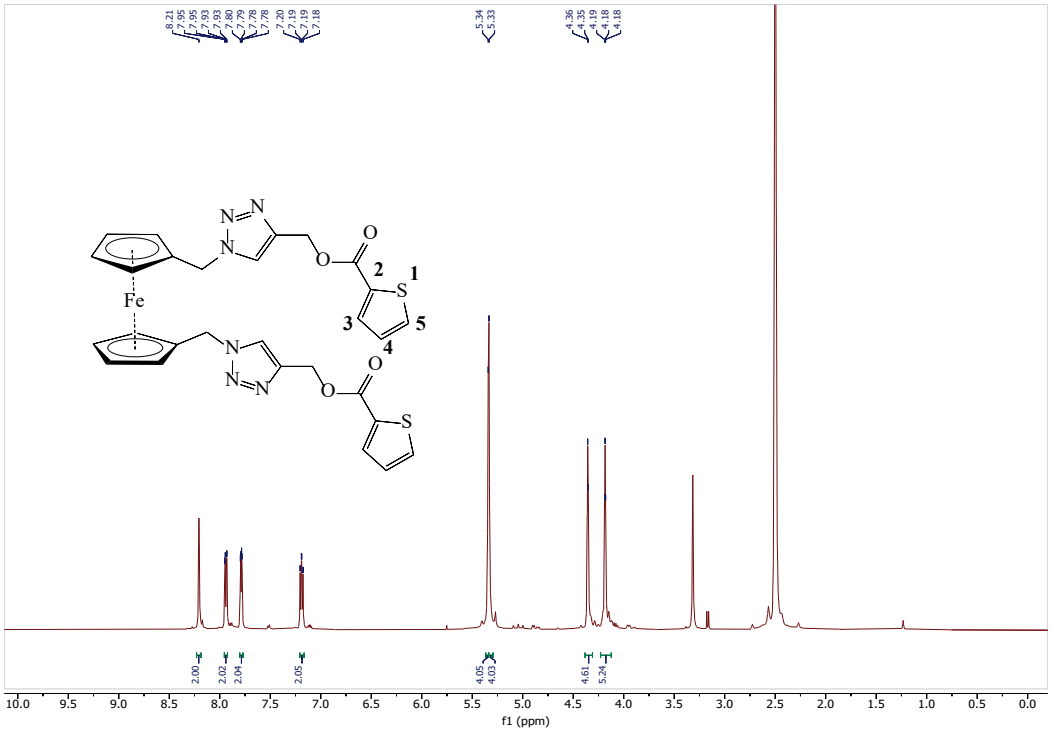


**Figure S20.** a) $^{1}$H NMR and b) $^{13}$C NMR spectra of compd. **9a**

**a)**




**b)**

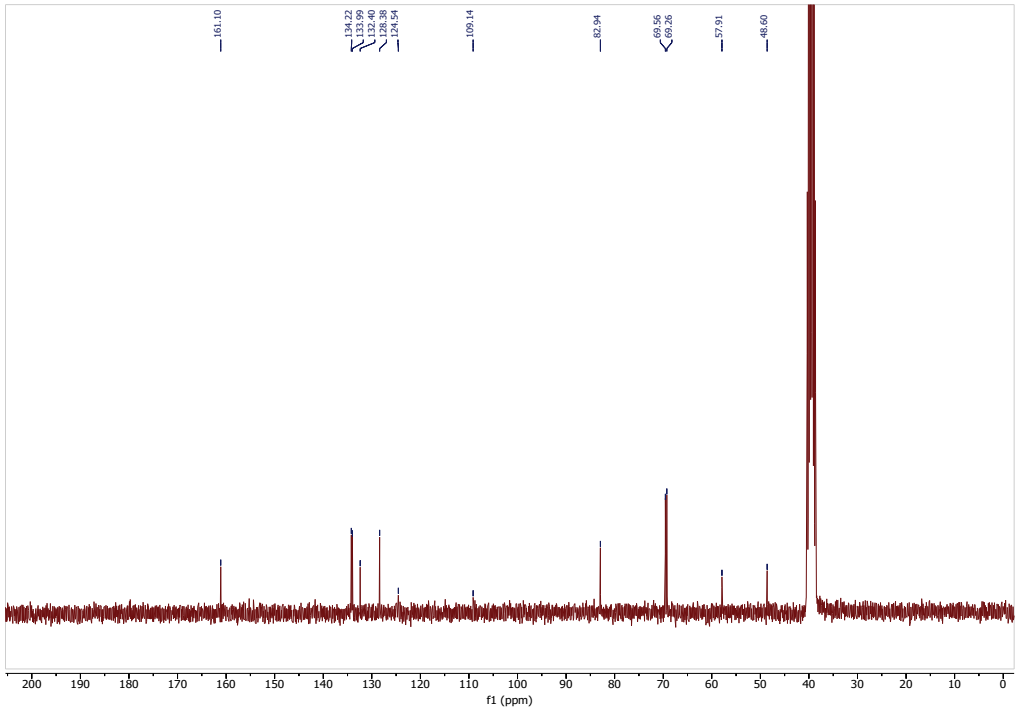
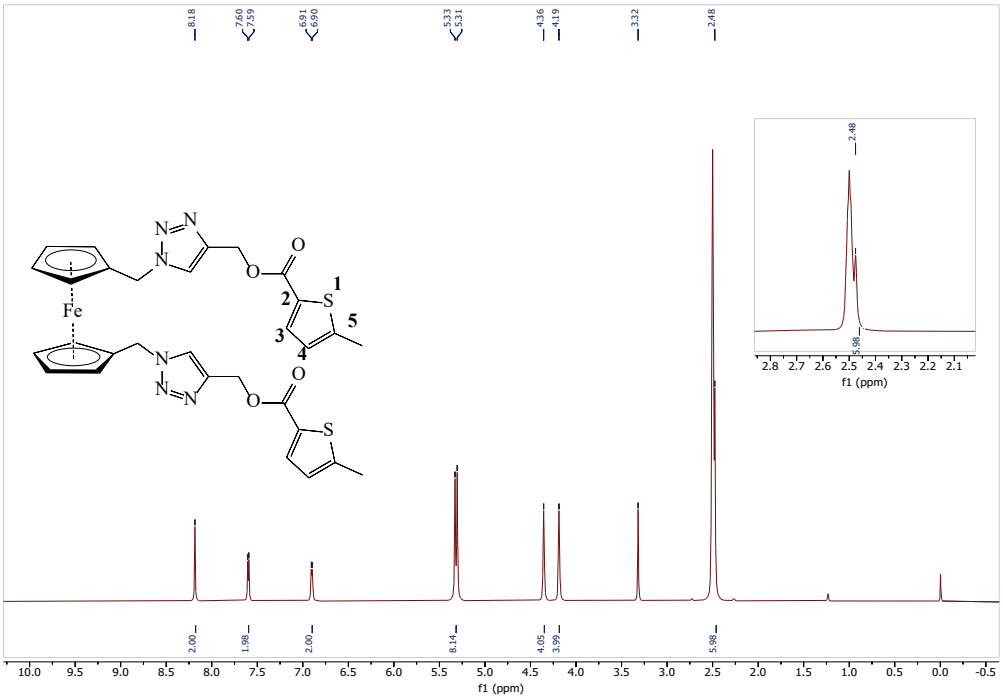


**Figure S21.** a) $^{1}$H NMR and b) $^{13}$C (APT) NMR spectra of compd. **9b**

**a)**




**b)**

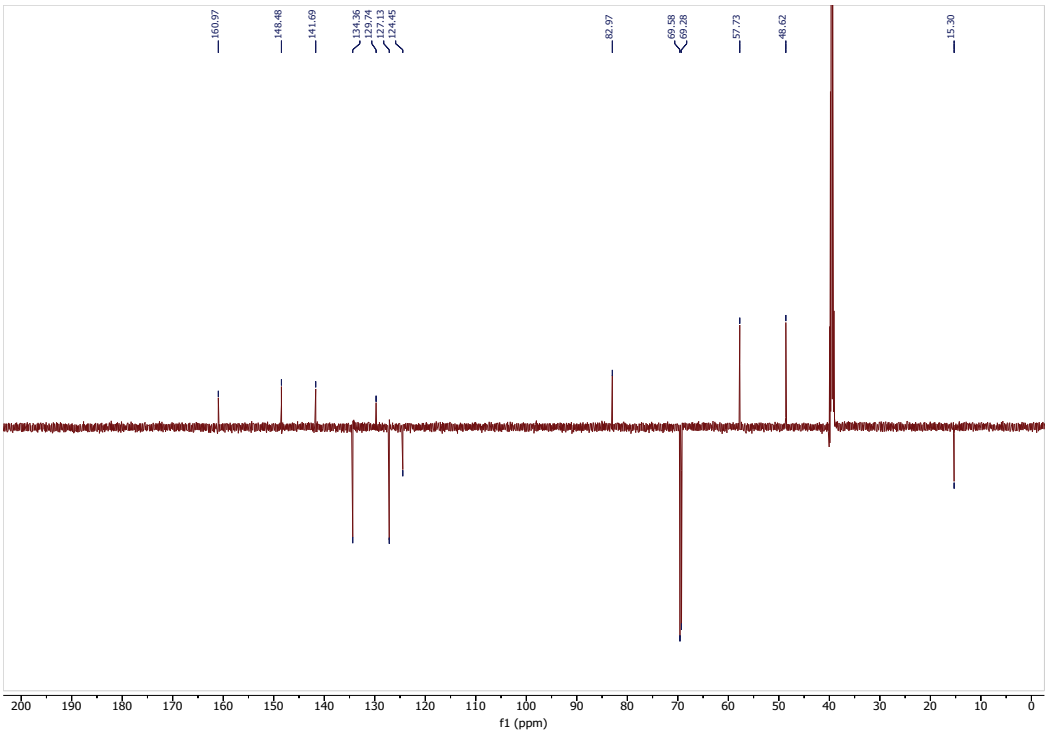
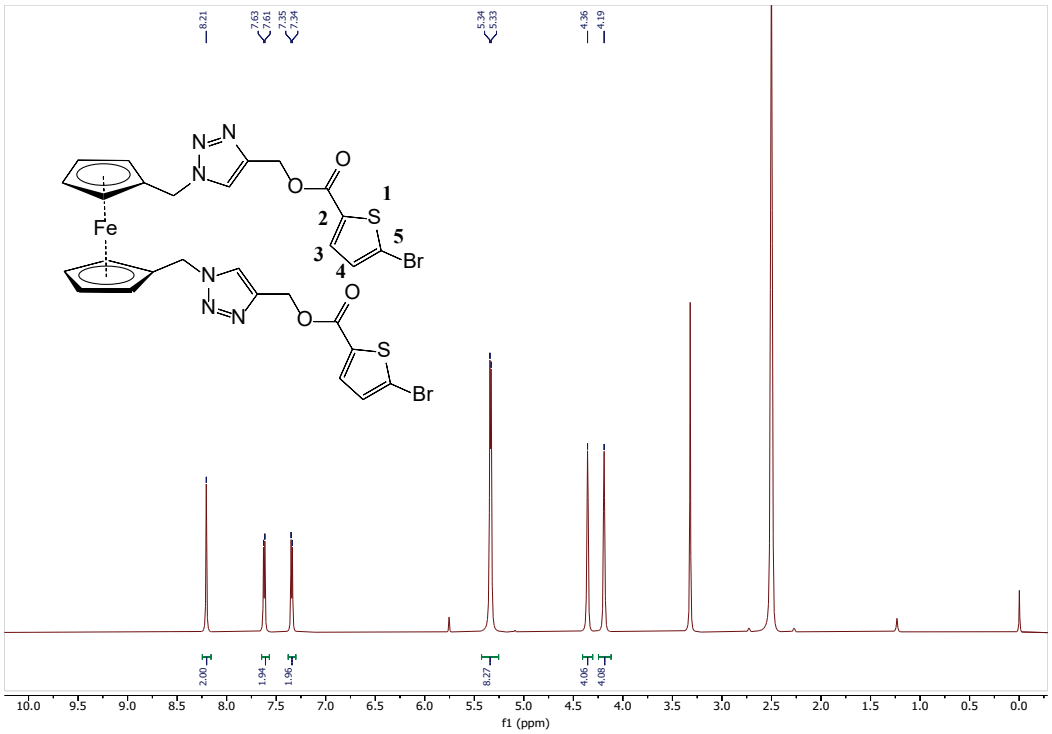


**Figure S22.** a) $^{1}$H NMR and b) $^{13}$C (APT) NMR spectra of compd. **9c**

**a)**




b)

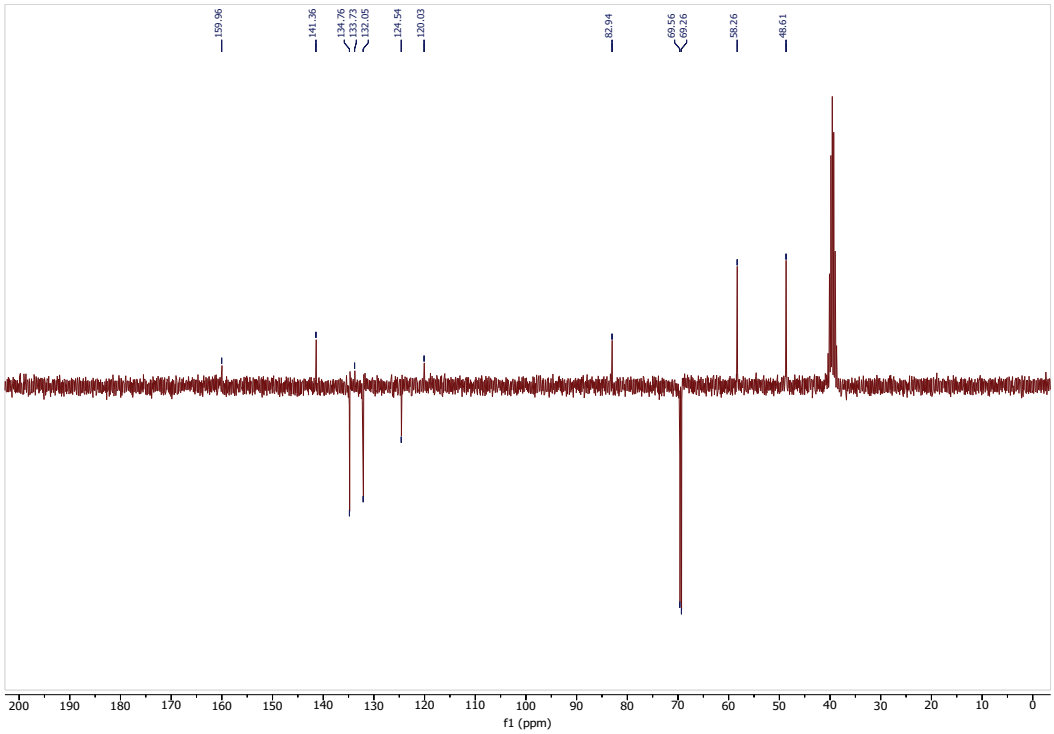
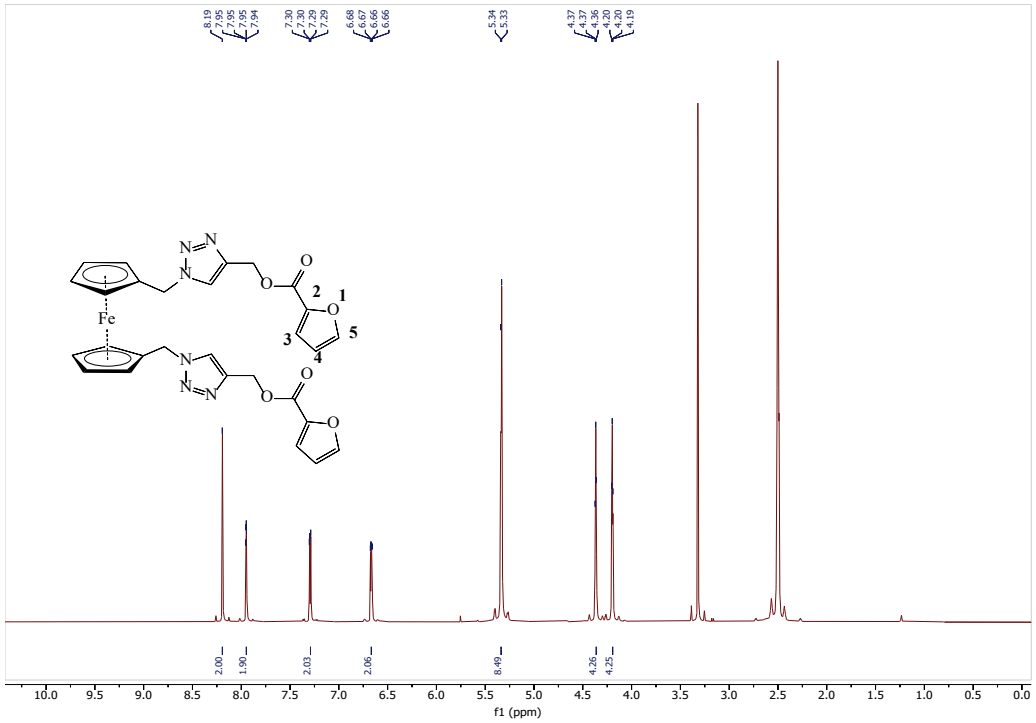


**Figure S23.** a) $^{1}$H NMR and b) $^{13}$C NMR spectra of compd. **9d**

**a)**




**b)**

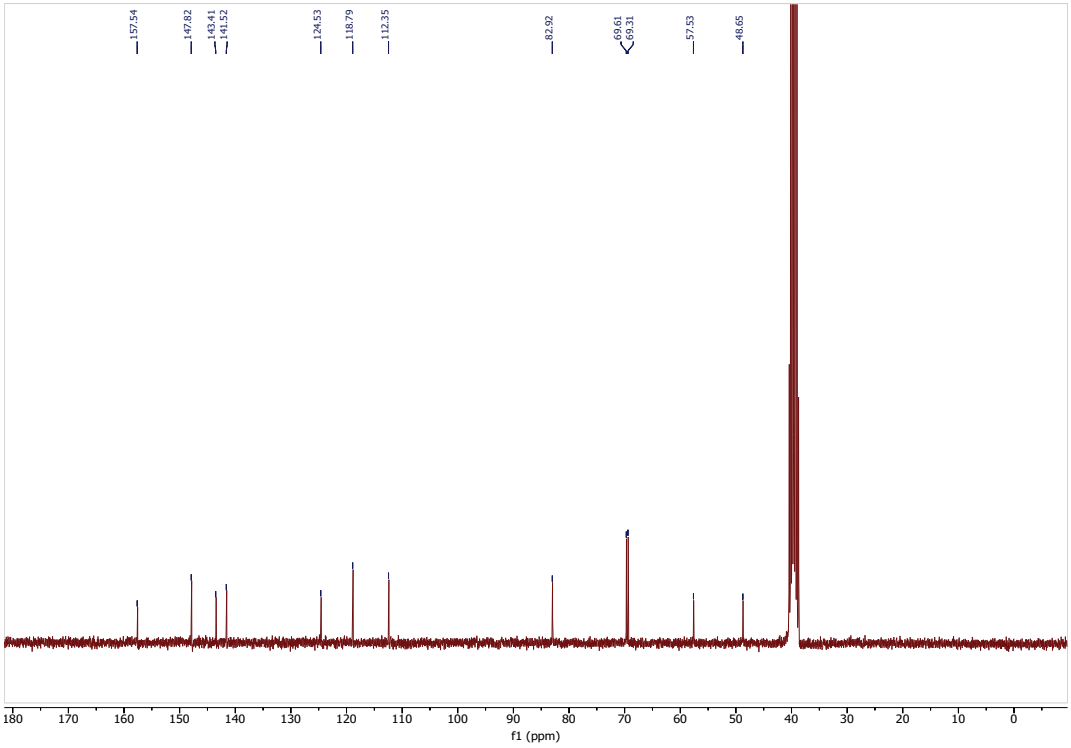
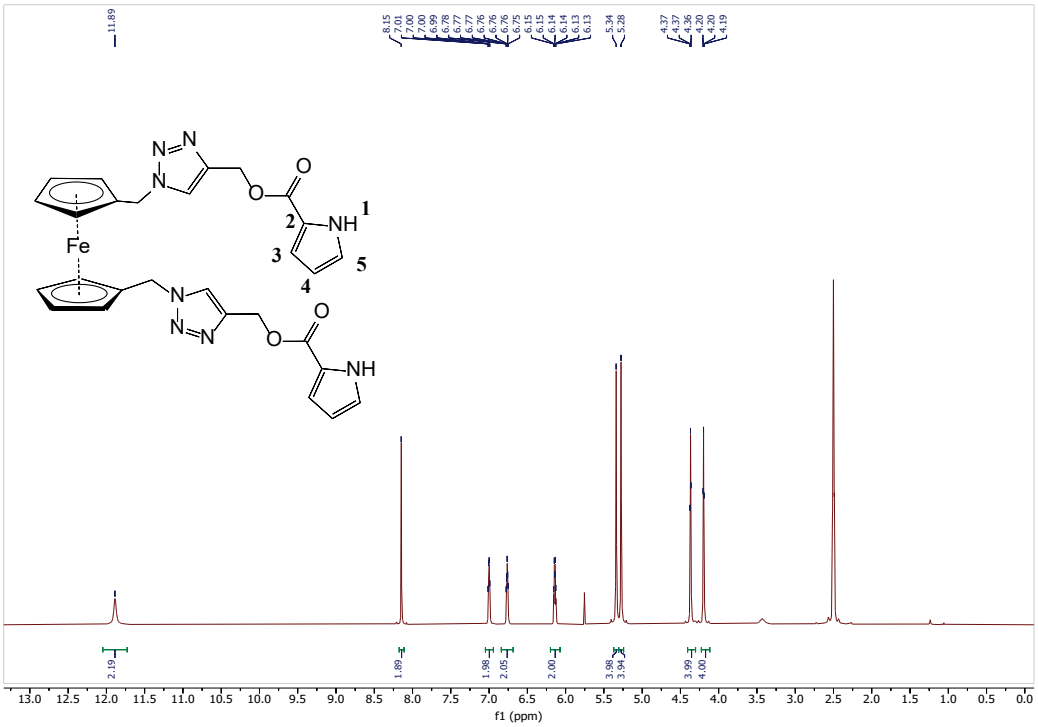


**Figure S24.** a) $^{1}$H NMR and b) $^{13}$C NMR spectra of compd. **9e**

**a)**




**b)**

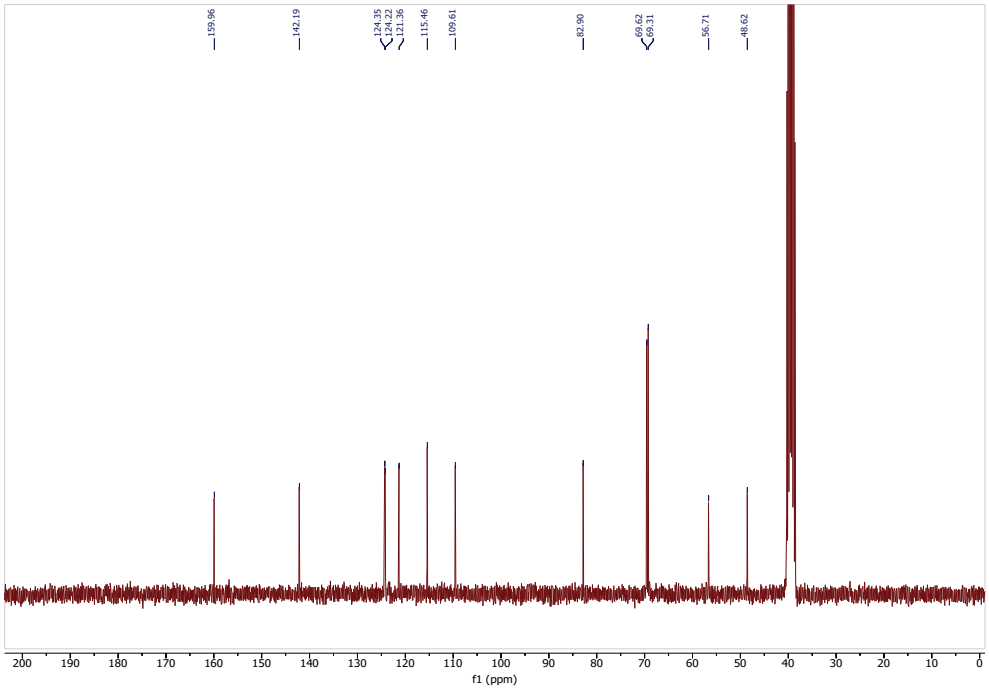
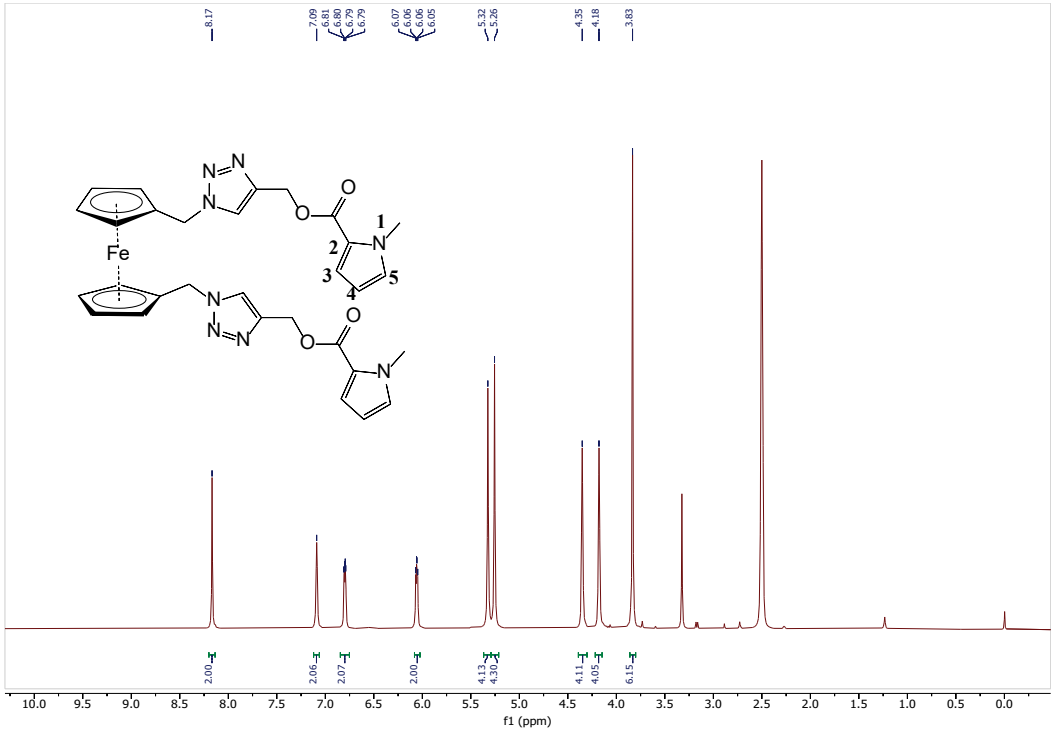
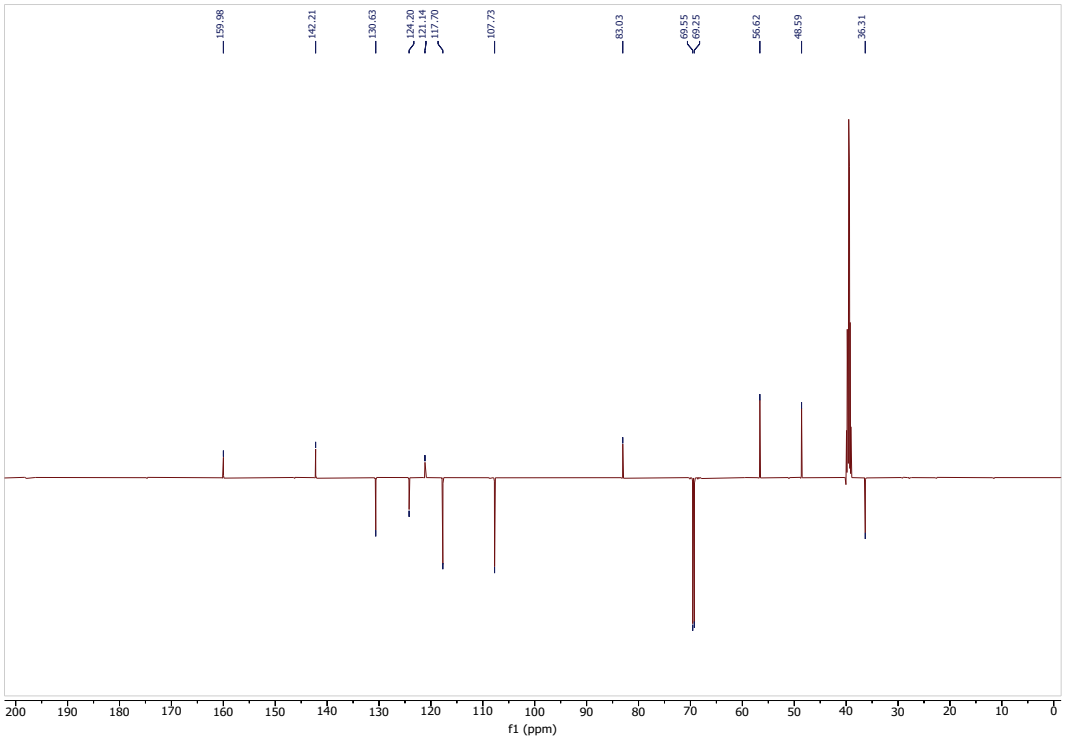


**Figure S25.** a) $^{1}$H NMR and b) $^{13}$C (APT) NMR spectra of compd. **9f**

**a)**




b)



## 2. HRMS spectra of novel compounds 5a–c, 6a–f, 8a–c, 9a–f

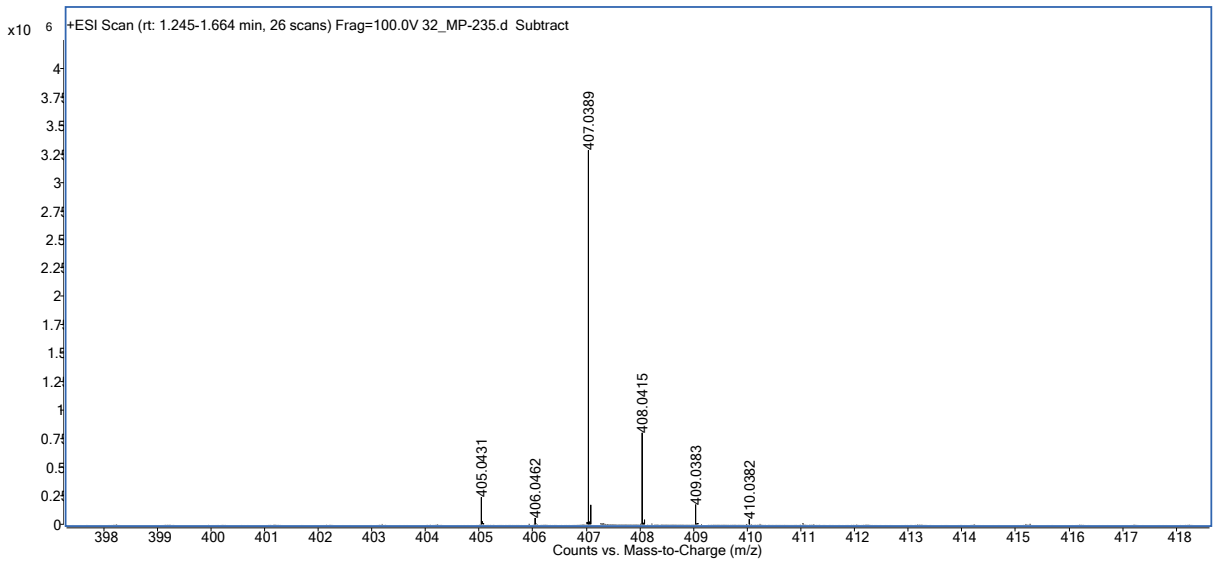



Figure S26. HRMS spectra of compound **5a**.

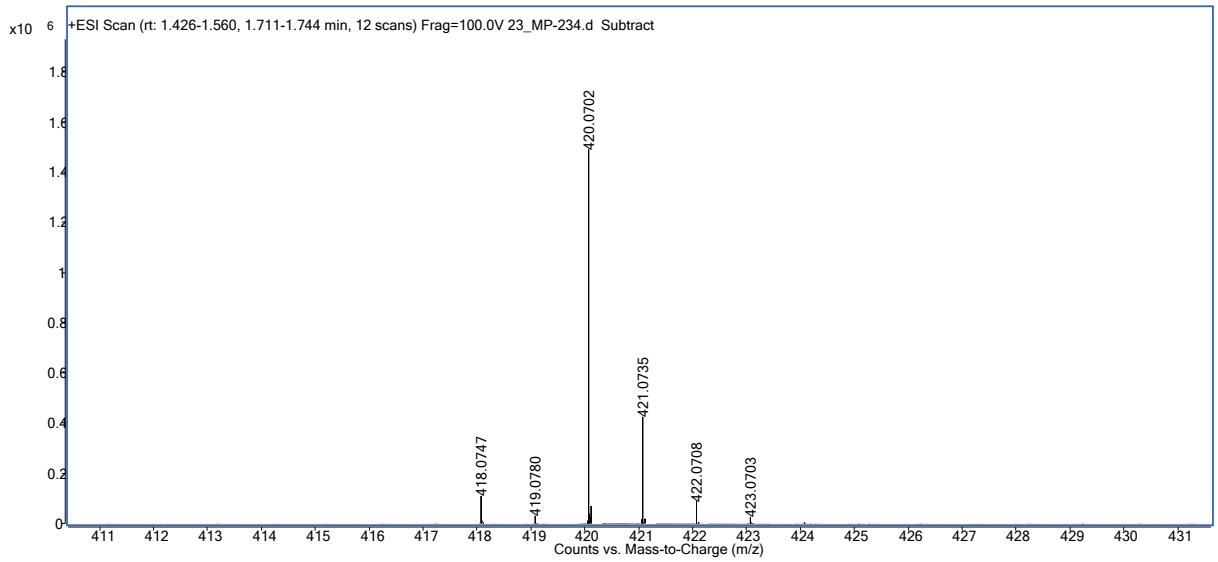



Figure S27. HRMS spectra of compound **5b**.

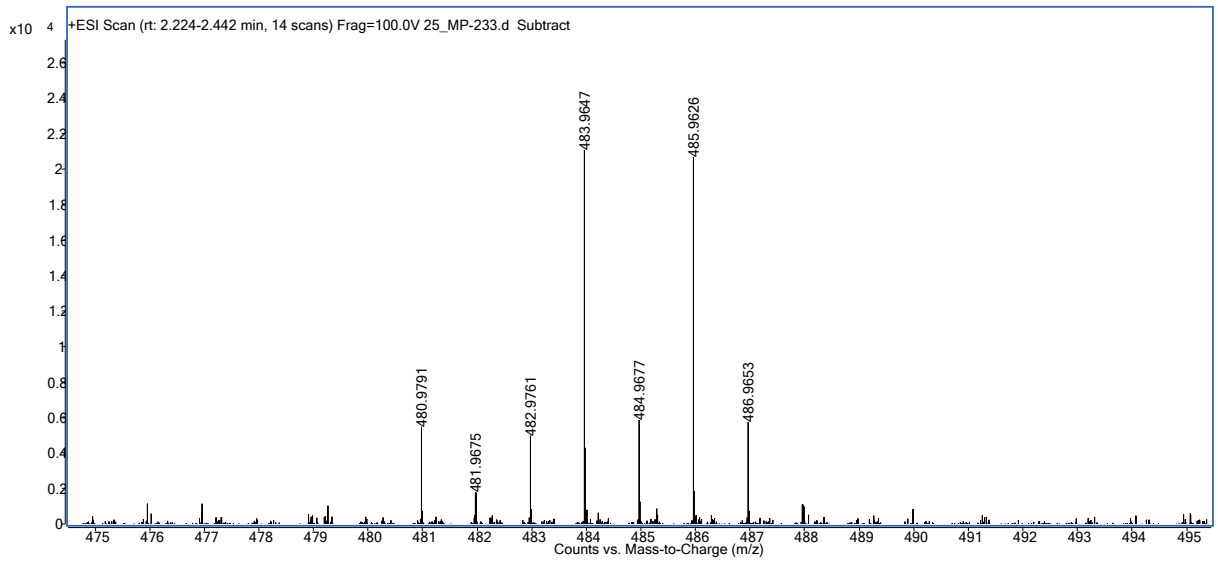



Figure S28. HRMS spectra of compound **5c**.

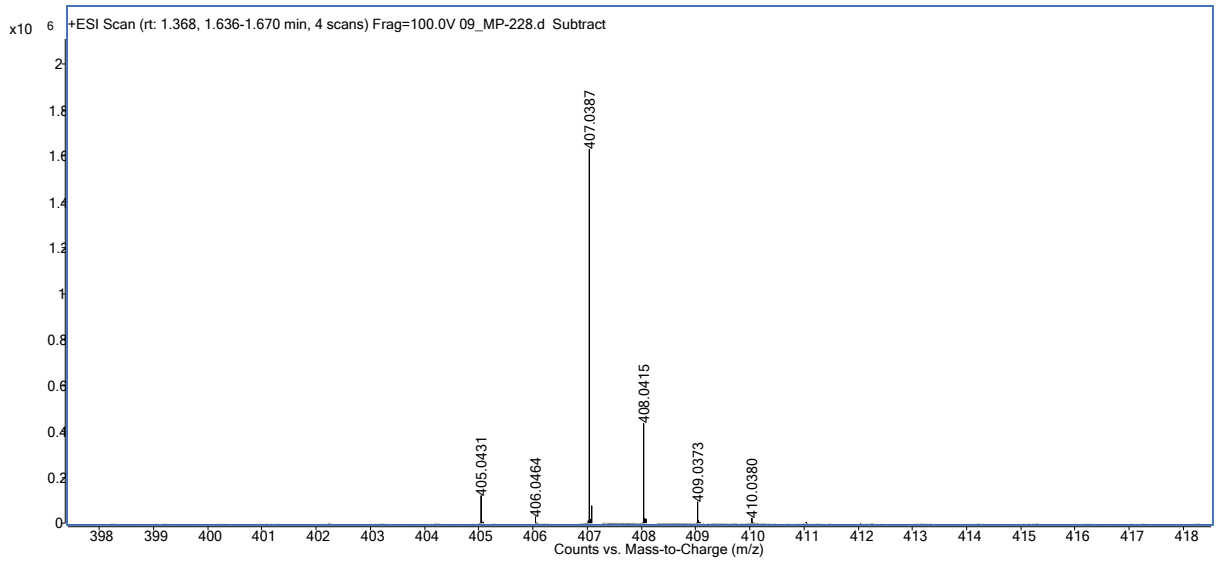



Figure S29. HRMS spectra of compound **6a**.

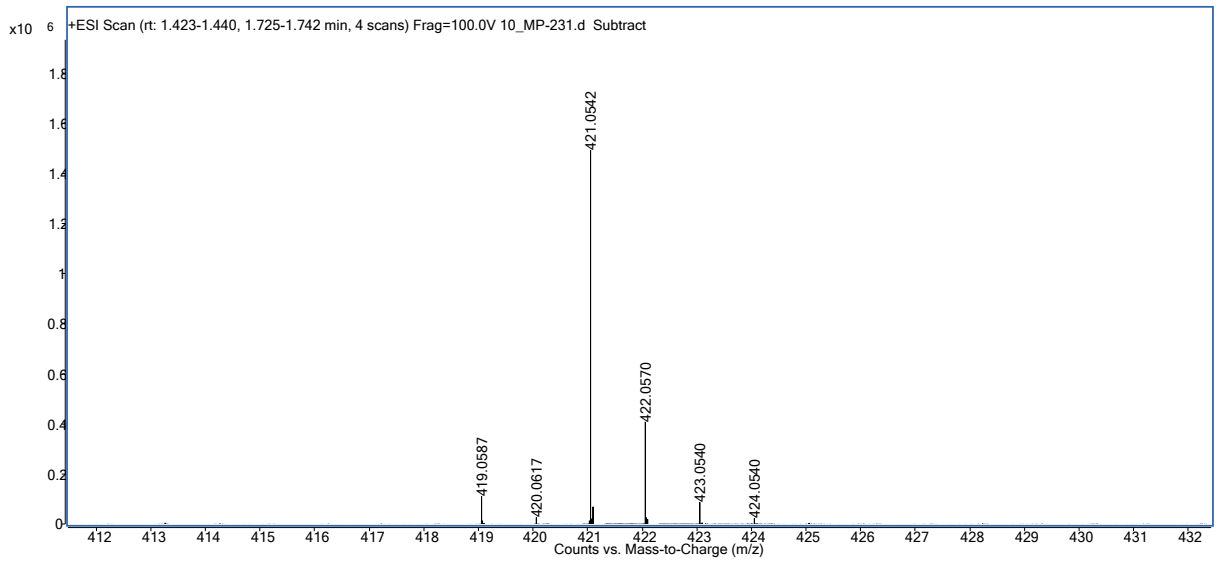



Figure S30. HRMS spectra of compound **6b**.

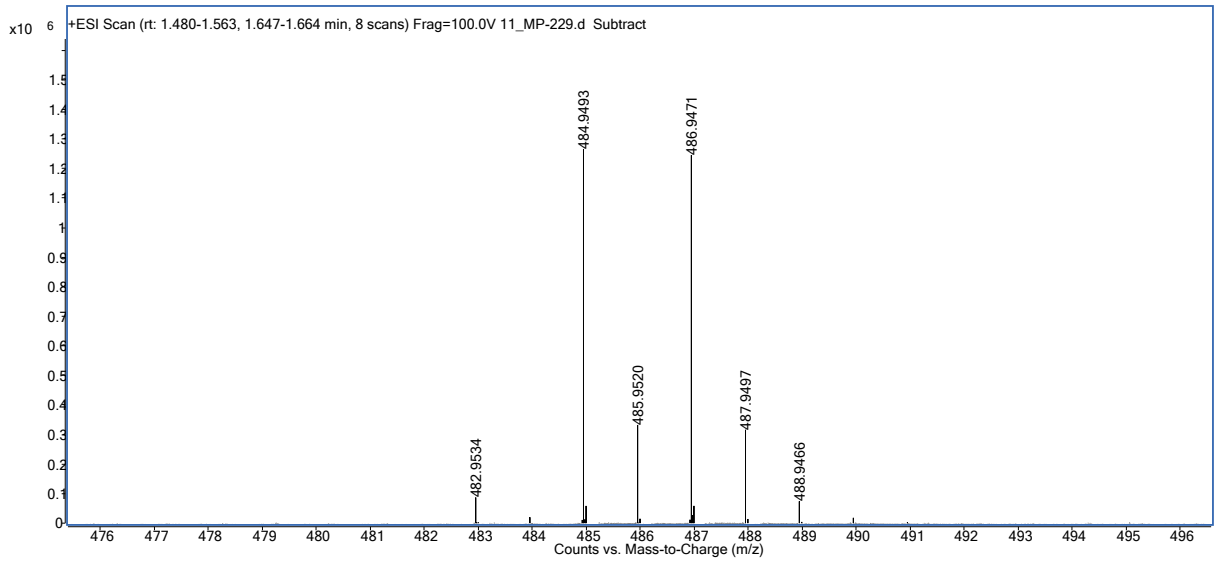



Figure S31. HRMS spectra of compound **6c**.

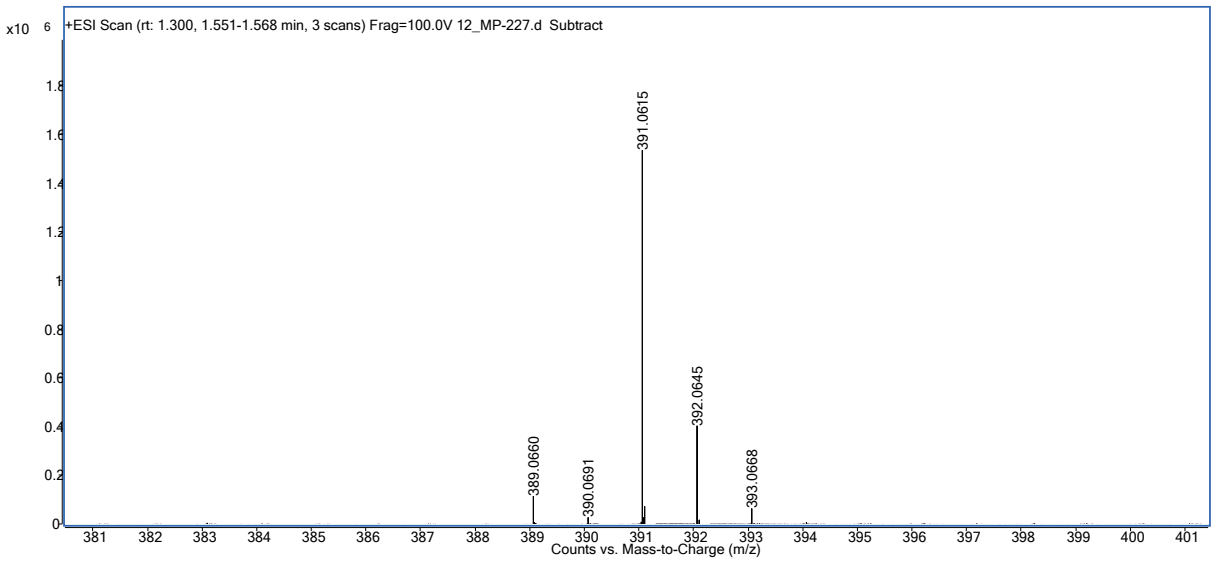



Figure S32. HRMS spectra of compound **6d**.

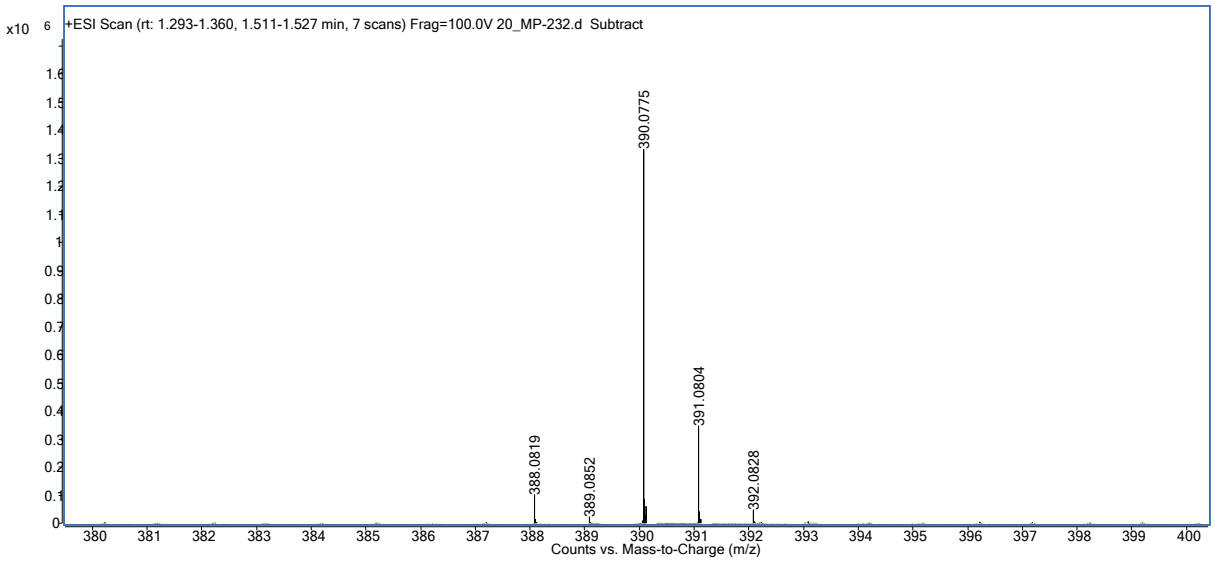



Figure S33. HRMS spectra of compound **6e**.

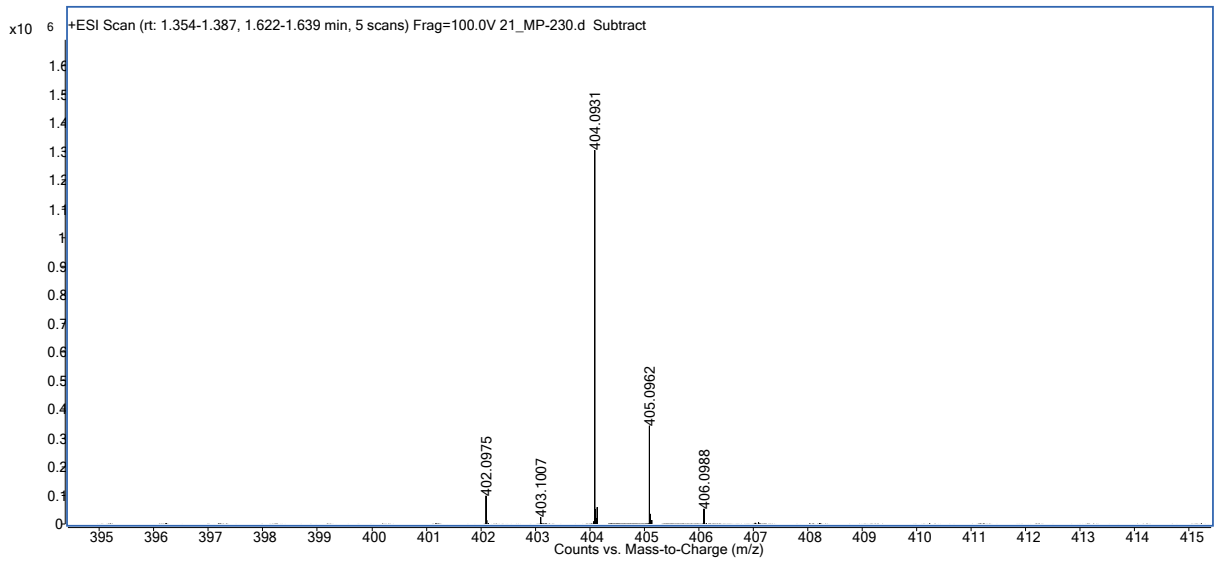



Figure S34. HRMS spectra of compound **6f**.

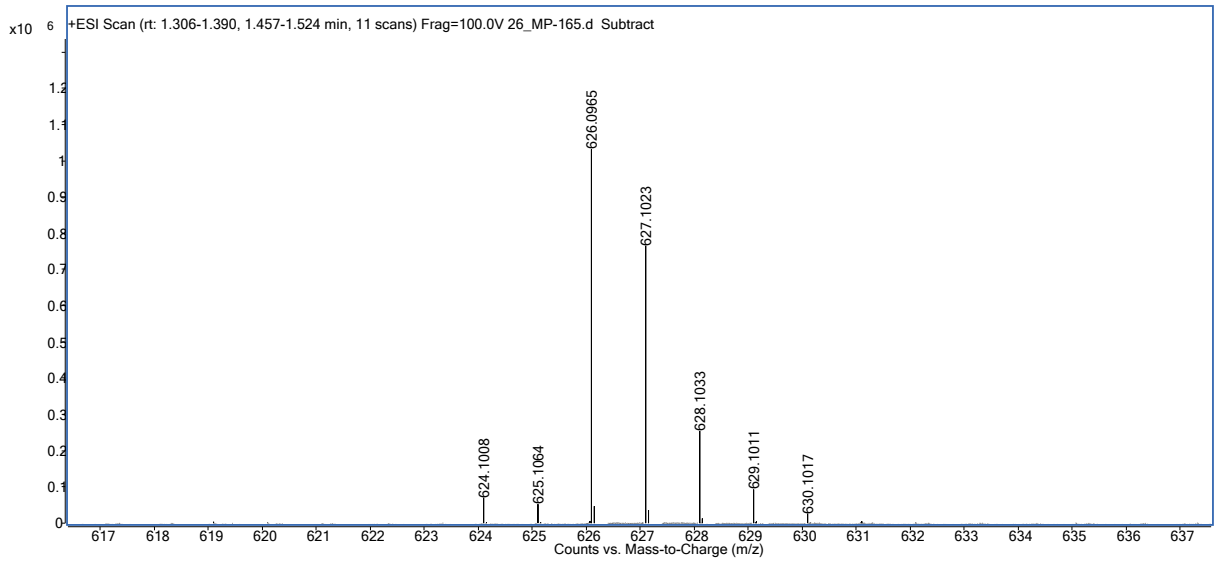



Figure S35. HRMS spectra of compound **8a**.

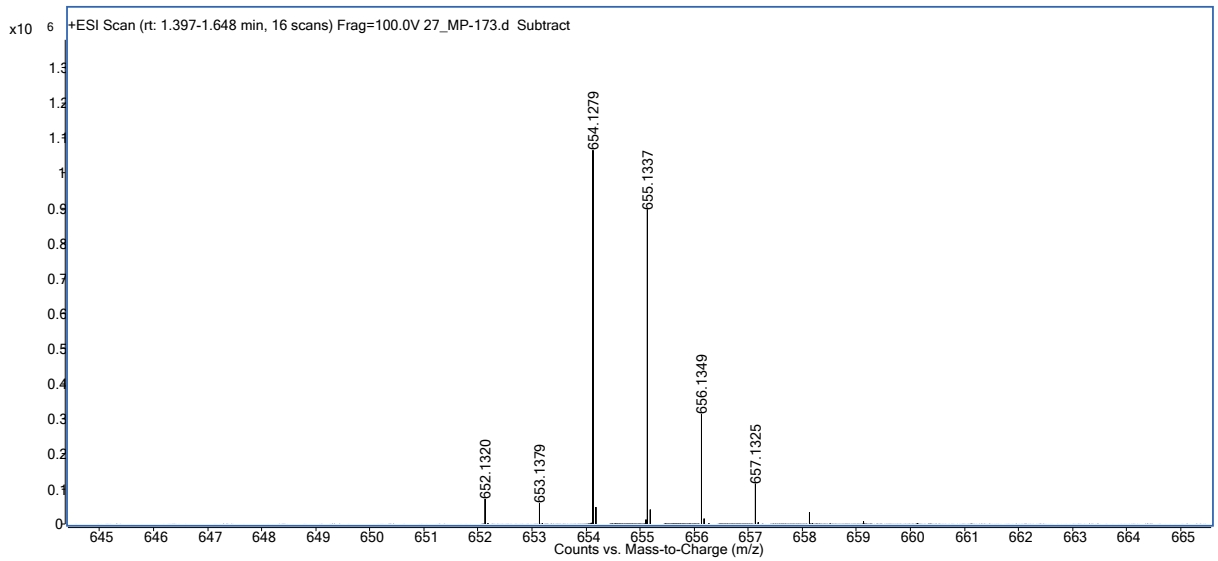



Figure S36. HRMS spectra of compound **8b**.

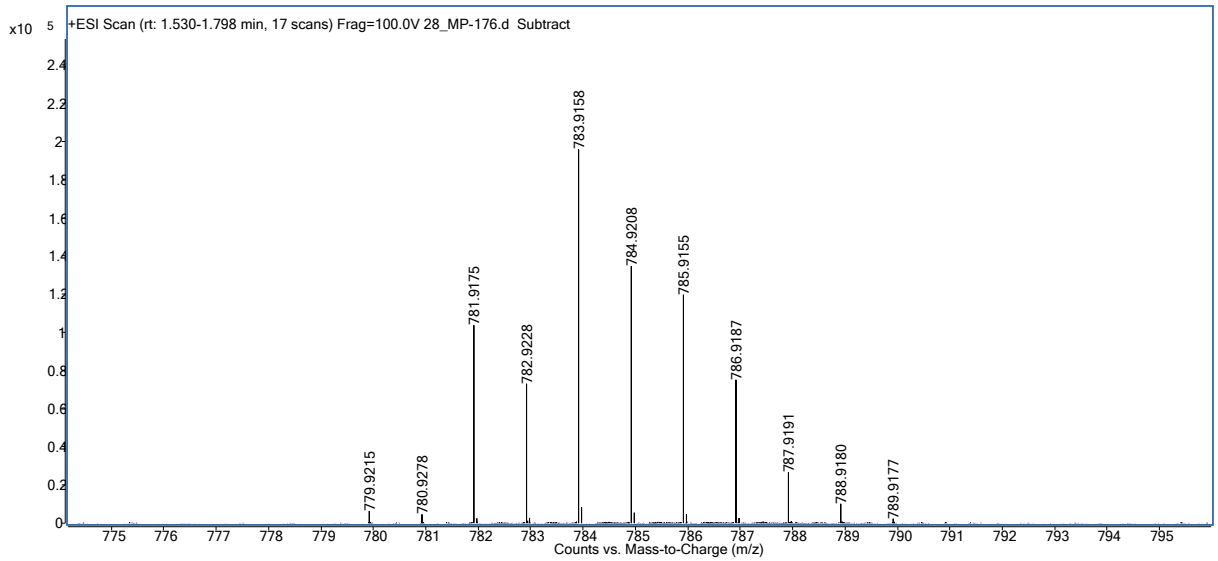



Figure S37. HRMS spectra of compound **8c**.

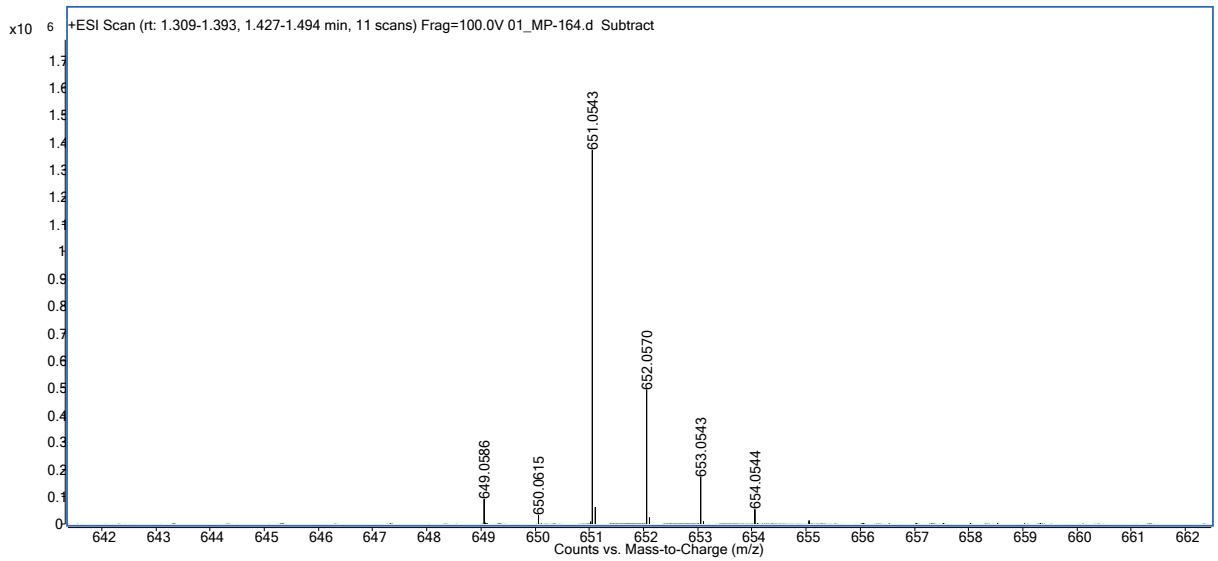



Figure S38. HRMS spectra of compound **9a**.

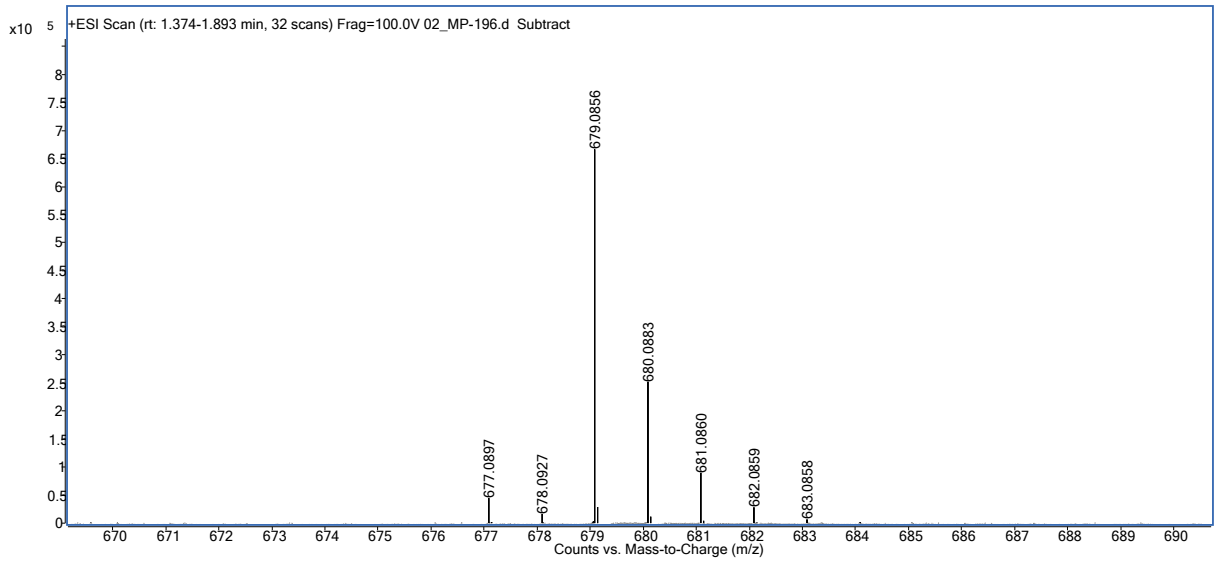



Figure S39. HRMS spectra of compound **9b**.

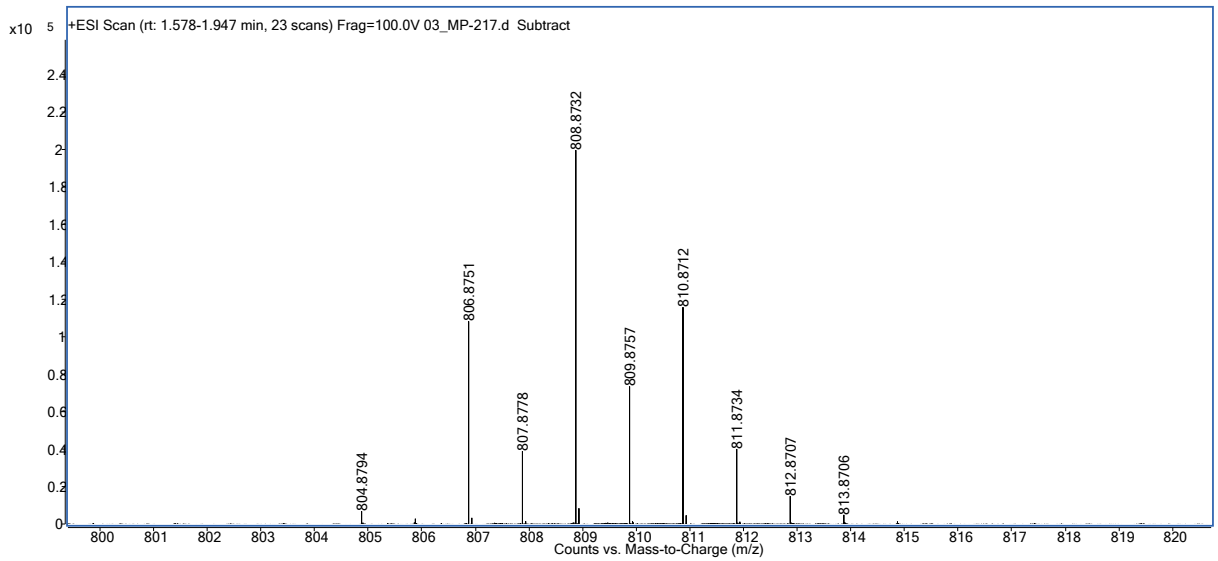



Figure S40. HRMS spectra of compound **9c**.

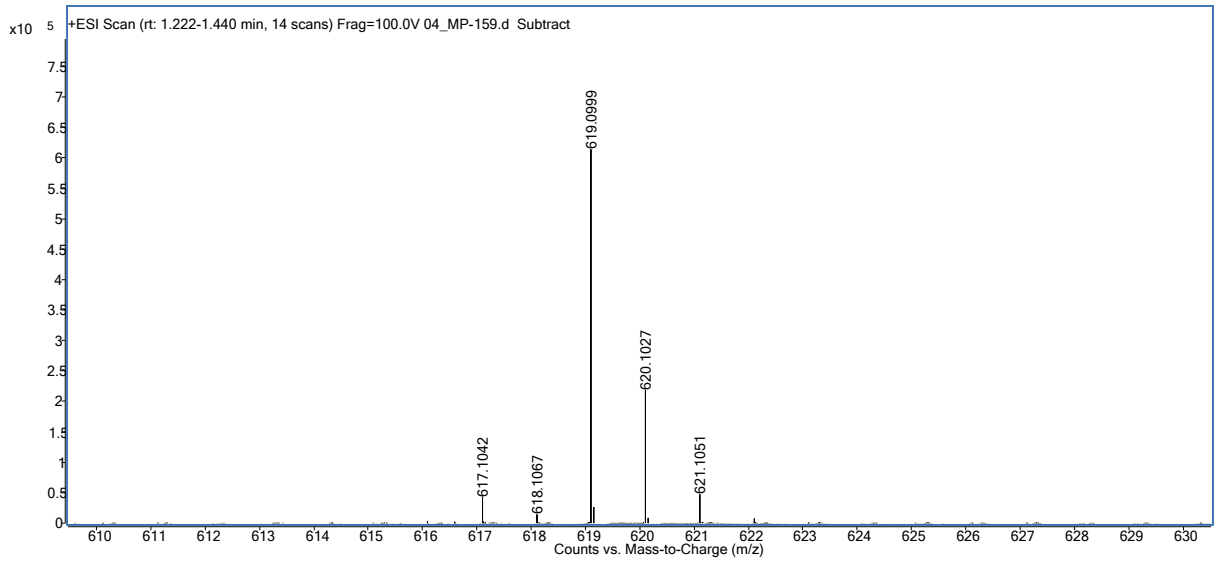



Figure S41. HRMS spectra of compound **9d**.

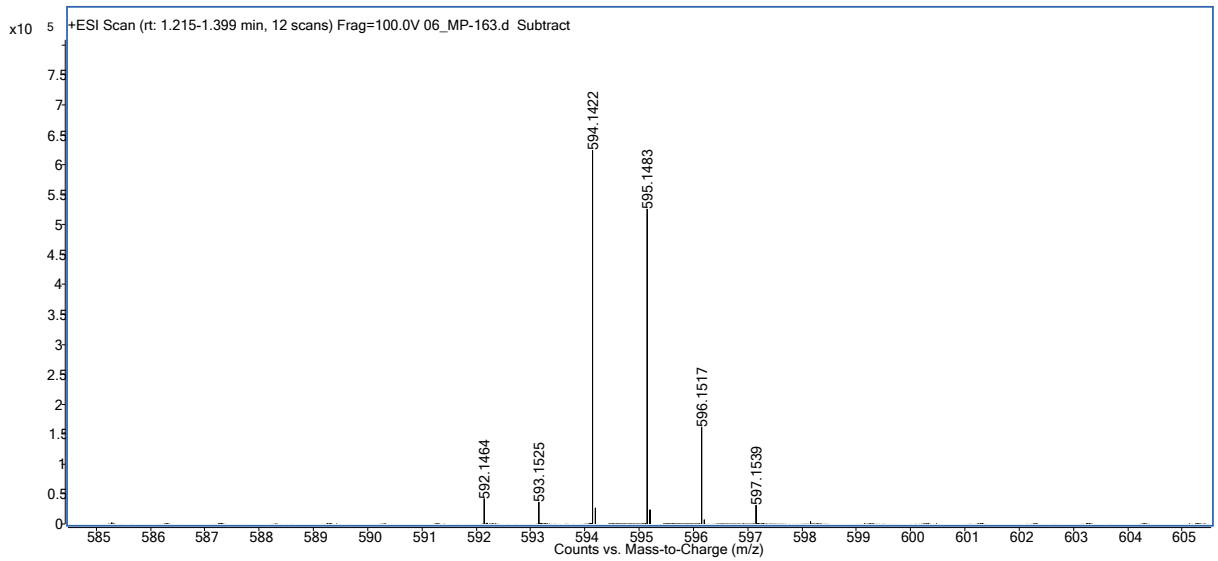



Figure S42. HRMS spectra of compound **9e**.

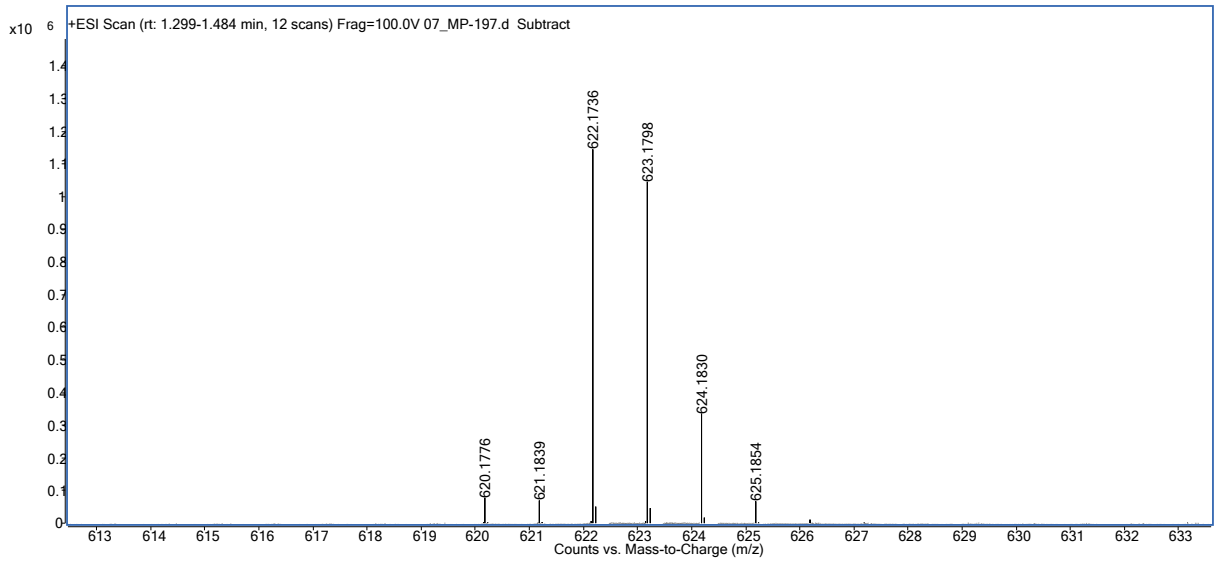



Figure S43. HRMS spectra of compound **9f**.

## 3. X-ray crystal structure studies of compounds **5b, 6c**, **6d**, and **6f**

### 3.1 Experimental

Single crystal X-ray data for **5b, 6c**, **6d**, and **6f** were collected at 297 K on a Rigaku XtaLAB Synergy-S diffractometer equipped with a HyPix-6000HE detector using mirror-monochromatized $CuK_\alpha$ radiation ($\lambda$ = 1.54184 Å). The *CrysAlisPro* program was used for the data collection and processing.[1] The intensities were corrected for absorption using analytical (**6c**), numerical (**6f**), and multi-scan (**5b** and **6d**) absorption correction methods.[1] The structures were solved using dual-space algorithm with *SHELXT*[2] and refined by full-matrix least-squares calculations based on $F^2$ using *SHELXL*–2018/3[3] within *Olex*2[4] program package. Hydrogen atoms were included in calculated positions, and were refined with riding coordinates or as rotating group, with *SHELXL*–2018/3 defaults.[3] The crystal of **6d** was recognized and refined as a 2-component twin. The scale factor BASF was refined to a final value of 0.526(2). Details of crystal data, data collection and structure refinement are summarized in Table S1. The *PLATON*[5] and *Mercury*[6] programs were used for structure analysis and figures preparation, respectively.

Table S1. Crystal data and structure refinement parameters of **5b**, **6c**, **6d**, and **6f**.

| | **5b** | **6c** | **6d** | **6f** |
|---|---|---|---|---|
| Formula | $C_{20}H_{20}FeN_4OS$ | $C_{19}H_{16}BrFeN_3O_2S$ | $C_{19}H_{17}FeN_3O_3$ | $C_{20}H_{20}FeN_4O_2$ |
| Formula weight | 420.31 | 486.17 | 391.20 | 404.25 |
| Crystal system | monoclinic | monoclinic | monoclinic | triclinic |
| Space group | *P* c | *P* $2_1$/c | *P* $2_1$/c | *P* -1 |
| Unit cell dimensions | | | | |
| *a* / Å | 5.71847(10) | 21.8716(5) | 22.4016(8) | 9.7314(4) |
| *b* / Å | 16.2487(3) | 8.4624(2) | 7.3533(3) | 9.8317(5) |
| *c* / Å | 10.10656(16) | 10.30233(19) | 10.6569(4) | 10.0426(5) |
| $\alpha$ / ° | 90 | 90 | 90 | 67.507(4) |
| $\beta$ / ° | 94.7150(16) | 91.0779(19) | 92.826(3) | 88.244(3) |
| $\gamma$ / ° | 90 | 90 | 90 | 89.381(3) |
| *V* / Å$^3$ | 935.90(3) | 1906.48(7) | 1753.32(11) | 887.33(7) |
| *Z* | 2 | 4 | 4 | 2 |
| $D_{calc.}$ / g cm$^{-3}$ | 1.491 | 1.694 | 1.482 | 1.513 |
| Absorption coef. $\mu$ / mm$^{-1}$ | 7.645 | 9.975 | 7.107 | 7.001 |
| $\theta$ range / ° | 5.167 - 67.982 | 4.043 - 67.996 | 3.951 - 67.989 | 4.546 - 67.982 |
| Collected reflections No. | 5780 | 13743 | 6094 | 9471 |
| Independent refl. No. / $R_{Int.}$ | 2310 / 0.0326 | 3468/ 0.0325 | 6094 / - | 3226 / 0.0404 |
| Reflections No. $I \geq 2\sigma(I)$ | 2243 | 2951 | 5247 | 3012 |
| Data[a]/Restraints/Parameters | 2310 / 2 / 245 | 3468 / 0 / 244 | 6094 / 0 / 236 | 3226 / 0 / 245 |
| Goodness-of-fit on $F^2$, *S* | 1.029 | 1.059 | 1.058 | 1.053 |
| *R* [$I \geq 2\sigma(I)$] / *R* [all data] | 0.0249 / 0.0258 | 0.0530 / 0.0602 | 0.0680 / 0.0749 | 0.0346 / 0.0367 |
| *wR* [$I \geq 2\sigma(I)$] / *wR* [all data] | 0.0620 / 0.0624 | 0.1614 / 0.1685 | 0.2120 / 0.2272 | 0.0935 / 0.0949 |
| Max. / min. el. density / e Å$^{-3}$ | 0.189 / -0.262 | 1.604 / -0.623 | 0.547 / -0.603 | 0.460 / -0.335 |

[a] Equal to independent reflections.

3.2. Results and discussion

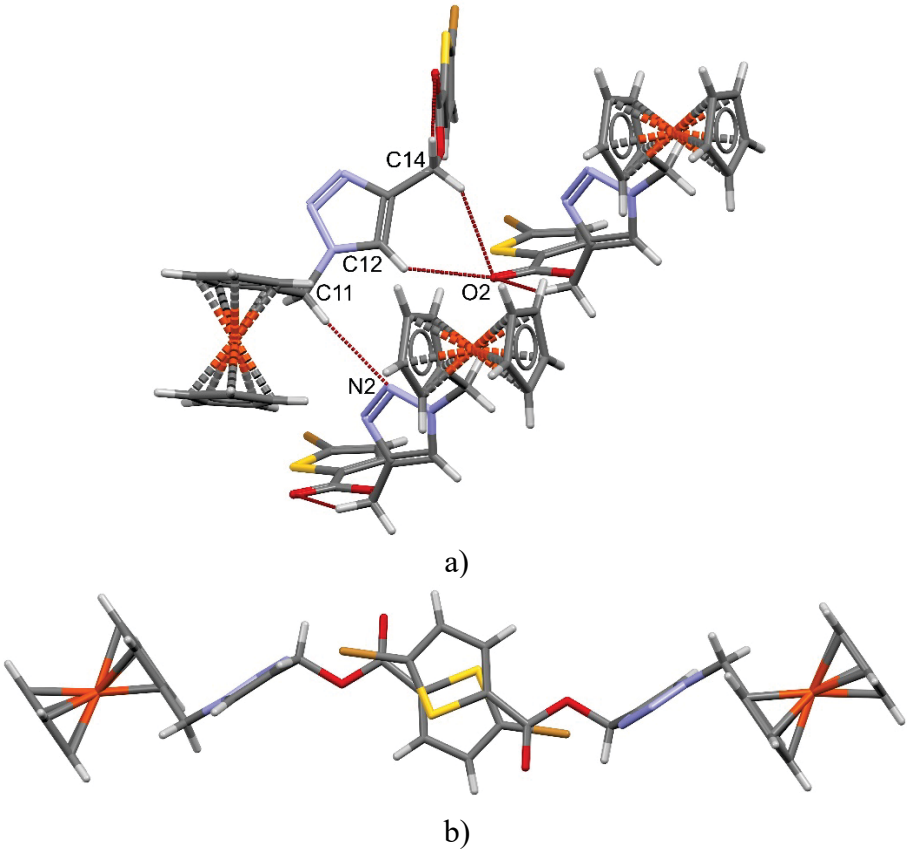



Figure S44. Partial view of molecular packing of **6c**, showing C−H···N and C−H···O hydrogen bonds (a) and one π···π interaction between thiophene rings of neighbouring molecules (b). Hydrogen bonds are indicated by red dashed lines.

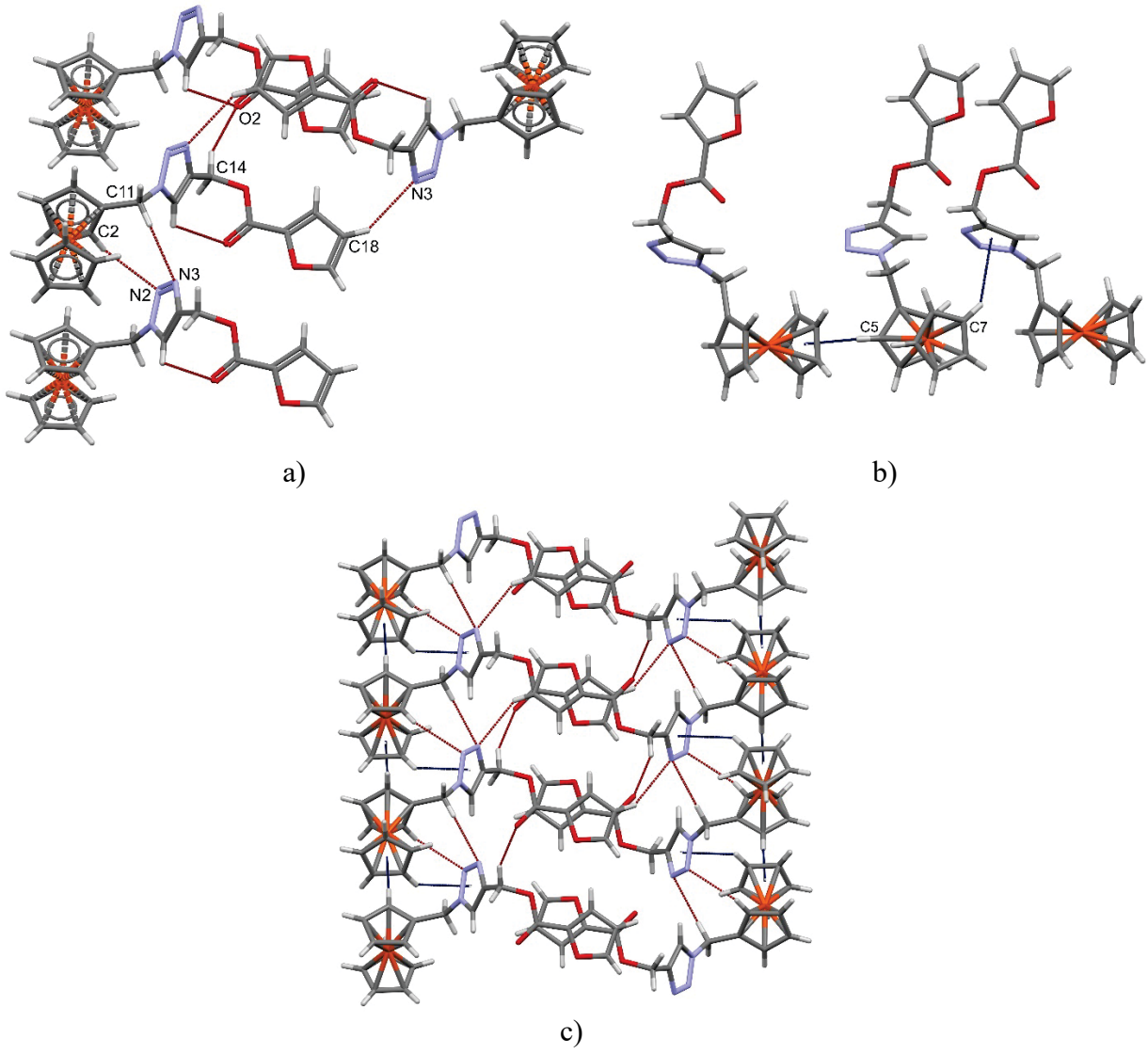
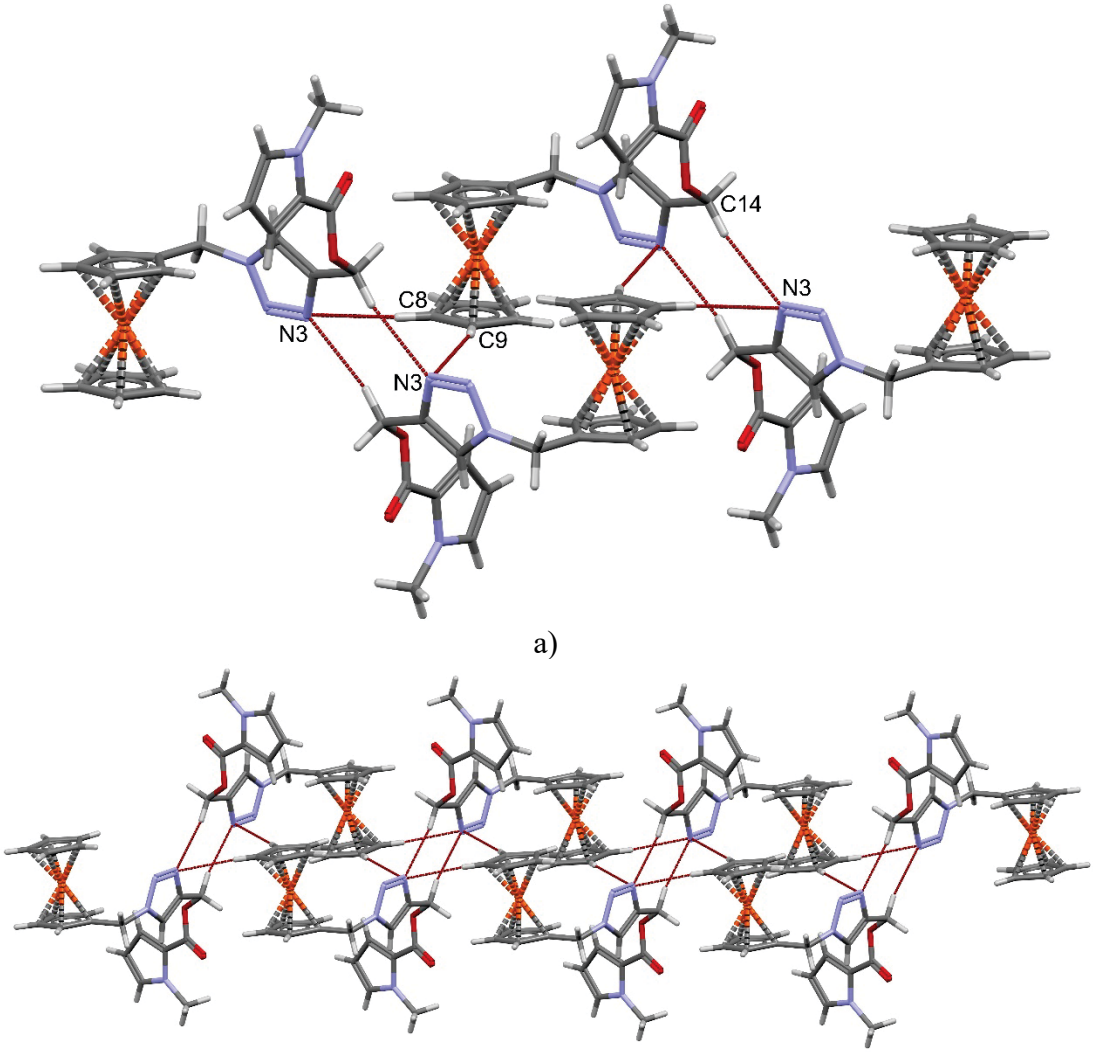


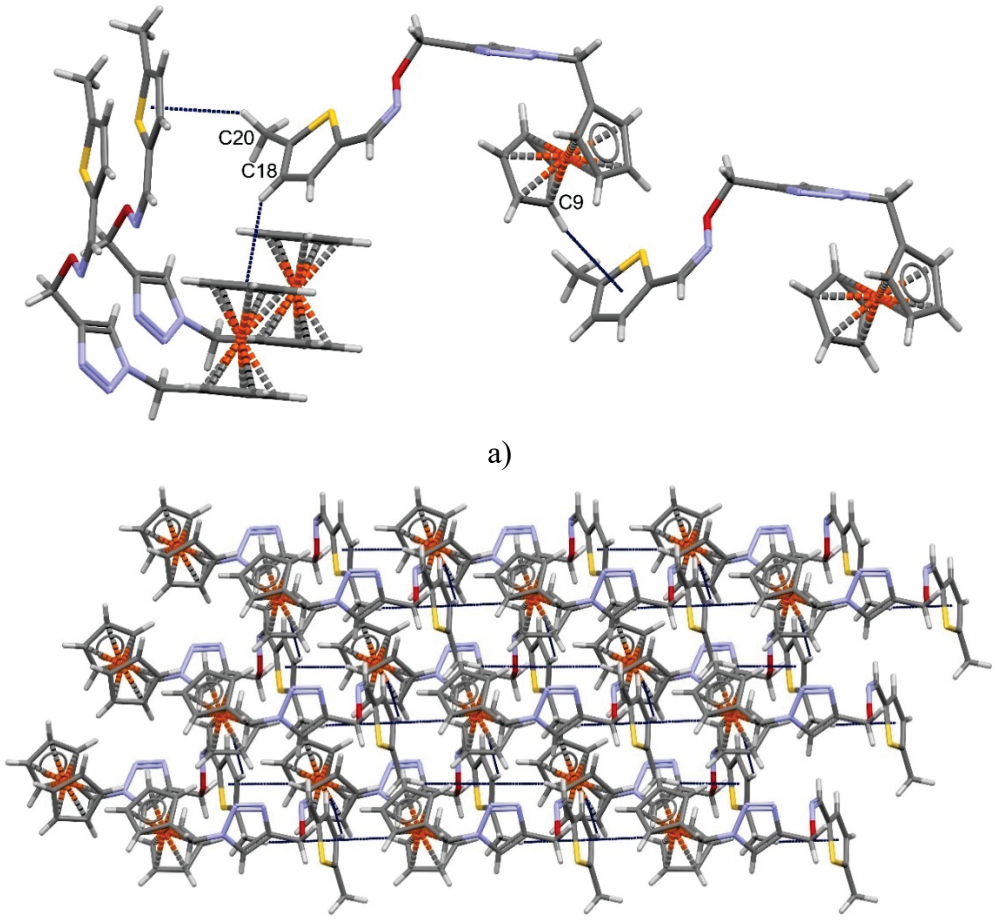

Figure S45. Partial view of molecular packing of **6d**, showing C−H···N and C−H···O hydrogen bonds (a), C−H···π interactions (b), and two-dimensional network formed by these and two π···π interactions. Hydrogen bonds are indicated by red dashed lines, while C−H···π interactions by blue dashed lines.




a)

b)

Figure S46. Partial view of molecular packing of **6f**, showing C−H···N hydrogen bonds (a), and one-dimensional chain motif generated by these interactions (b). Hydrogen bonds are indicated by red dashed lines.




a)

b)

Figure S47. Partial view of molecular packing of **5b**, showing C−H···π interactions (a), and two-dimensional network formed by these interactions (b). C−H···π interactions are indicated by blue dashed lines.

Table S2. Selected torsion angles in **5b**, **6c**, **6d**, and **6f**.

| Torsion angle | **5b** | **6c** | **6d** | **6f** |
|---|---|---|---|---|
| C12–C13–C14–O1 | 82.6(4) | 108.9(6) | –79.7(7) | 48.2(3) |
| C13–C14–O1–C15 | --- | 114.2(5) | 81.6(6) | –88.9(2) |
| C14–O1–C15–C16 | --- | –176.3(4) | 176.0(4) | 171.20(16) |
| O1–C15–C16–C17 | --- | 4.4(7) | –2.0(8) | –13.0(3) |
| C13–C14–O1–N4 | 71.3(4) | --- | --- | --- |
| C14–O1–N4–C15 | 169.0(3) | --- | --- | --- |
| O1–N4–C15–C16 | –1.7(6) | --- | --- | --- |
| N4–C15–C16–C17 | –177.7(4) | --- | --- | --- |

Table S3. Dihedral angles between rings in **5b**, **6c**, **6d**, and **6f**.

| Dihedral angle / $^{o}$ | **5b** | **6c** | **6d** | **6f** |
|---|---|---|---|---|
| Triazole / $Cp_1$ [a] | 66.89(18) | 88.3(3) | 65.2(3) | 77.13(12) |
| Heterocyclic / $Cp_1$ [a] | 88.52(18) | 86.1(3) | 43.2(3) | 85.72(14) |
| Heterocyclic / triazole | 58.97(18) | 86.1(3) | 63.4(3) | 86.10(14) |

[a] $Cp_1$ is the C1–C5 cyclopentadienyl ring.

Table S4**.** Intermolecular hydrogen-bonding geometries for **5b**, **6c**, **6d**, and **6f**.

| | D–H···A | D–H (Å) | H···A (Å) | D···A (Å) | D–H···A (°) | Symmetry codes |
|---|---|---|---|---|---|---|
| **5b** | C9–H9···*Cg*1[a] | 0.93 | 2.98 | 3.868(4) | 161 | 1+x, y, 1+z |
| | C18–H18···*Cg*2[a] | 0.93 | 2.85 | 3.621(4) | 141 | –1+x, 1–y, –1/2+z |
| | C20–H20A···*Cg*1[a] | 0.96 | 2.94 | 3.736(5) | 141 | x, 1–y, –1/2+z |
| **6c** | C11–H11A···N2 | 0.97 | 2.61 | 3.556(7) | 167 | x, 3/2–y, –1/2+z |
| | C12–H12···O2 | 0.93 | 2.61 | 3.332(6) | 135 | x, 1/2–y, –1/2+z |
| | C14–H14B···O2 | 0.97 | 2.72 | 3.487(7) | 137 | x, 1/2–y, –1/2+z |
| **6d** | C2–H2···N2 | 0.93 | 2.72 | 3.478(6) | 140 | x, 3/2–y, 1/2+z |
| | C11–H11B···N3 | 0.97 | 2.54 | 3.437(6) | 153 | x, 3/2–y, 1/2+z |
| | C14–H14B···O2 | 0.97 | 2.48 | 3.378(7) | 154 | x, 5/2–y, –1/2+z |
| | C18–H18···N3 | 0.93 | 2.72 | 3.532(7) | 146 | 1–x, 2–y, –z |
| | C5–H5···*Cg*2[a] | 0.93 | 2.74 | 3.640(5) | 164 | x, 1/2–y, –1/2+z |
| | C7–H7···*Cg*3[a] | 0.93 | 2.93 | 3.717(7) | 144 | x, 3/2–y, 1/2+z |
| **6f** | C8–H8···N3 | 0.93 | 2.71 | 3.619(3) | 168 | –1+x, y, z |
| | C9–H9···N3 | 0.93 | 2.71 | 3.576(4) | 155 | 1–x, 1–y, 2–z |
| | C14–H14A···N3 | 0.97 | 2.61 | 3.555(3) | 166 | 2–x, 1–y, 2–z |
| | C2–H2···*Cg*4[a] | 0.93 | 2.75 | 3.579(3) | 149 | 1–x, 1–y, 1–z |

[a] Ring centroids: *Cg*1=S1/C16–C19; *Cg*2=C6–C10; *Cg*3=N1–N3/C12/C13; *Cg*4=N4/C16–C19.

Table S5. π···π interactions geometries for **5b**, **6c**, **6d**, and **6f**.

| | Ring 1···Ring 2[a] | Cg···Cg (Å) | $\alpha$ (°) | CgI_Perp (Å) | Slippage (Å) | Symmetry codes |
|---|---|---|---|---|---|---|
| **5b** | Cg1···Cg2 | 3.8238(19) | 5.42(18) | 3.6902(12) | 1.004 | x, 2–y, –1/2+z |
| | Cg2···Cg1 | 3.8236(19) | 5.42(18) | 3.6896(14) | 1.002 | x, 2–y, 1/2+z |
| **6c** | *Cg*3···*Cg*3 | 3.791(3) | 0.0(3) | 3.559(2) | 1.306 | 1–x, –y, 1–z |
| **6d** | *Cg*4···*Cg*4 | 4.008(4) | 6.1(4) | 3.593(3) | 1.412 | 1–x, –1/2+y, 1/2–z |
| | *Cg*4···*Cg*4 | 4.007(4) | 6.1(4) | 3.750(3) | 1.776 | 1–x, 1/2+y, 1/2–z |
| **6f** | *Cg*2···*Cg*2 | 3.8266(13) | 0.00(12) | 3.5913(9) | 1.321 | 1–x, 1–y, 1–z |

[a] Ring centroids: *Cg*1=N1–N3/C12/C13; *Cg*2=C1–C5; *Cg*3=S1/C16–C19; *Cg*4=O3/C16–C19.

## 4. References


[1] Rigaku Oxford Diffraction, *CrysAlisPro* Software System, Version 1.171.42.49. Oxford, UK, 2022.

[2] G. M. Sheldrick, *Acta Crystallogr.* **2015**, *A71*, 3–8.

[3] G. M. Sheldrick, *Acta Crystallogr.* **2015**, *C71*, 3–8.

[4] O. V. Dolomanov, L. J. Bourhis, R. J. Gildea, J. A. K. Howard, H. Puschmann, *J. Appl. Cryst*. **2009**, *42*, 339–341.

[5] A. L. Spek, *Acta Crystallogr.* **2009**, *D65*, 148–155.

[6] C. F. Macrae, P. R. Edgington, P. McCabe, E. Pidcock, G. P. Shields, R. Taylor, M. Towler, J. van de Streek, *J. Appl. Crystallogr*. **2006**, *39*, 453–457.